Elsevier Editorial System(tm) for Journal of Food Engineering

Manuscript Draft

Manuscript Number: JFOODENG-D-16-01783R1

Title: Comparison between conventional and ultrasound-assisted techniques for extraction of anthocyanins from grape pomace. Experimental results and mathematical modeling

Article Type: Research Article

Keywords: anthocyanins; grape pomace; conventional solvent extraction; ultrasound-assisted extraction; first-principles modeling; mass transport coefficients

Corresponding Author: Dr. Maria Agustina Agustina Reinheimer, PhD

Corresponding Author's Institution: CAIMI - UTN-CONICET

First Author: Mónica Bonfigli

Order of Authors: Mónica Bonfigli; Ezequiel Godoy, PhD; Maria Agustina Agustina Reinheimer, PhD; Nicolás J Scenna, PhD

Abstract: Conventional and ultrasound assisted extraction of anthocyanins from grape pomace are here analyzed and compared. Mathematical modeling is used firstly to represent the extraction process and determine the associated mass transport parameters, and afterwards, to obtain useful predictions on how the system behaves under different operating conditions. The mathematical model here developed is based on first-principles, aided by , in order to more accurately describe the underlying phenomena that govern the extraction process behavior. Extraction of anthocyanins from grape pomace is performed using a hydro alcoholic solution as solvent, and experimental runs at different temperatures were carried out for both conventional and ultrasound-assisted techniques. A good agreement between experimental and computed extraction yields was achieved as the reported statistical parameters indicate. Obtained results highlight the performance differences between both processes, and pinpoint which variables impact the most in the extraction yield.

***Cover Letter**

To: Editor of *Journal of Food Engineering*

Subject: Submission of manuscript “Comparison between conventional and ultrasound-assisted techniques for extraction of anthocyanins from grape pomace. Experimental results and mathematical modeling”

Dear Sir,

Please find annexed with this letter the revised version of the manuscript “Comparison between conventional and ultrasound-assisted techniques for extraction of anthocyanins from grape pomace. Experimental results and mathematical modeling” for evaluation and publication, if accepted, in *Journal of Food Engineering*.

The authors state that this paper has not been published previously, it is not under consideration for publication elsewhere, and if accepted it will not be published elsewhere in substantially the same form, in English or in any other language, without the written consent of the Publisher.

I look forward to hearing from you. Yours sincerely,

María Agustina Reinheimer

***Highlights (for review)**

>> Opportunities identification in the recovery of anthocyanins from grape pomace

>> Comparison of conventional and ultrasound-assisted extraction techniques

>> Process representation by mathematical modeling

>> Application of first principles equations and semi-empirical correlations

>> Prediction of the system performance under different operating conditions

Comparison between conventional and ultrasound-assisted techniques for extraction of anthocyanins from grape pomace. Experimental results and mathematical modeling

M. Bonfigli, E. Godoy, M.A. Reinheimer*, N. J. Scenna

Centro de Aplicaciones Informáticas y Modelado en Ingeniería (CAIMI),
Universidad Tecnológica Nacional, Facultad Regional Rosario (UTN, FRRo),
Zeballos 1346, S2000BQA Rosario, Argentina

* Corresponding author.
E-mail address: *mareinheimer@santafe-conicet.gob.ar*

Abstract

Conventional and ultrasound assisted extraction of anthocyanins from grape pomace are here analyzed and compared. Mathematical modeling is used firstly to represent the extraction process and determine the associated mass transport parameters, and afterwards, to obtain useful predictions on how the system behaves under different operating conditions. The mathematical model here developed is based on first-principles, in order to more accurately describe the underlying phenomena that govern the extraction process behavior.

Extraction of anthocyanins from grape pomace is performed using a hydro alcoholic solution as solvent, and experimental runs at different temperatures were carried out for both conventional and ultrasound-assisted techniques. A good agreement between experimental and computed extraction yields was achieved as the reported statistical parameters indicate. Obtained results highlight the performance differences between both processes, and pinpoint which variables impact the most in the extraction yield.

Keywords: anthocyanins; grape pomace; conventional solvent extraction; ultrasound-assisted extraction; first-principles modeling; mass transport coefficients

Nomenclature

Symbols

AED	acoustic energy density (W/l)
C	anthocyanins concentration (mg/ml)
D	mass diffusivity (m^2/s)
k	global mass transfer coefficient (m/s)
K	distribution constant (-)
MW	molecular weight (kDa)
M	number of radial discretization points (-)
m	mass (kg)
N	number of temporal discretization points (-)
R	sample radius (m)
r	spherical radial coordinate (m)
s	specific surface for mass transfer (m^2/m^3)
T	temperature (^oC)
t	time (s)
Δt	temporal grid with (s)
v	agitation velocity (m/s)
V	volume (m^3)
V_m	molar volume (at the boiling point) (m^3/kmol)
Y	extraction yield (%)

Dimensionless groups

Re	Reynolds's number (-)
Sh	Sherwood's number (-)
Sc	Schmidt's number (-)

Greek symbols

ε	volume fraction of solvent (-)
δ	spatial grid width (m)
ρ	density (kg/m^3)
μ	viscosity (kg/ms^2)
φ	solvent association parameter (-)

Subscripts

0	at initial
a	anthocyanins
i	at interphase
β	solid particle
γ	solvent phase
f	at final time
p	particle

Acronyms

CSE	Conventional Solvent Extraction
UAE	Ultrasound-Assisted Extraction

1. Introduction

Grape pomace consists of the skin, stems, and seeds that remain after grapes processing in the wine industry, where large amounts of bagasse are generated. This by-product is usually discarded as natural waste or utilized as animal feed or compost (Monrad et al., 2010).

Furthermore, the wine lees obtained from red wine are a good source of anthocyanins that belong to a specific group of phenolic compounds. Polyphenols are chemical compounds that are characterized by a significant antioxidant capacity (Spigno and De Faveri, 2007), and their numerous health-benefiting properties, including oxidative stress reduction, free radical scavenging properties, assisting in cancer and disease risk reduction and cholesterol regulation (Stevenson and Hurst, 2007).

The extraction of bioactive components from vegetable by-products is an interesting way to increase the value of this waste product (Balasundram et al., 2006). Phenolic compounds can be extracted from plant-based materials by various extraction technologies and solvents, depending on their distribution in the plant matrix and chemical properties.

The conventional solvent extraction (CSE), which has been proposed for decades, requires prolonged extraction times and relatively large quantities of solvent. Therefore, various novel extraction techniques have been employed for the extraction of bioactive compounds from foods, including ultrasound-assisted extraction (Tao et al., 2014a), microwave-assisted extraction (Valdés et al., 2015) and supercritical fluid extraction (Meneses et al., 2015). Ultrasound-assisted extraction (UAE) can improve the extraction of heat-sensitive bioactive components by lower processing temperatures (Tao et al., 2014a), and is a more effective technique than conventional extraction (Both et al., 2014; He et al., 2016). The mechanical effects of ultrasound provide a greater

solvent penetration into cellular materials thus improving mass transfer, while the disruption of biological cell walls facilitates the release of its contents (Tao et al., 2014a). UAE has two main advantages compared with conventional extraction, which are reduced processing time and solvent volume usage, as shorter operating times are obtained compared with conventional methods (Veličković et al., 2006). However, there is a lack of published models describing the physics mechanisms for the internal and external mass transfer coefficients. This point will be further explained and addressed in the model here proposed.

In food engineering, it is important to implement mathematical models of extraction processes to facilitate process design, optimization and control, as well as to provide useful information for equipment scale-up. These models usually consist of a set of algebraic, partial and ordinary differential equations (DAEs), implemented via suitable spatial discretization methods (e.g. finite differences, method of lines, finite elements, etc.), resulting in highly non-linear problems.

Rigorous and detailed modeling is a difficult task due to the complexity of the underlying mechanisms, uncertainties about the measurement of food properties, and difficulty for the achievement of reliable experimental data. In fact, the combination of first principles models with experimental data through empirical relationships is a common practice in order to accurately describe food processing by mathematical modeling (Banga et al., 2003). Such semi-empirical correlations usually comprise the main mass transfer coefficients (distribution constant and solute diffusion in the food matrix) for a given range of extraction conditions (temperature, type of solvent, solid and solvent ratio, agitation speed).

In particular, numerous studies have addressed the antioxidant extraction process from a food matrix (Cheng et al., 2016; Qu et al., 2010; Yim et al., 2012) and also the

specific extraction of other compounds from different food products (Da Porto et al., 2013; Espinoza-Perez et al., 2007; Reinheimer et al., 2014). Most of them describe the internal mass transfer, using kinetic modeling and fitting, to predict the internal mass diffusion coefficient. Meanwhile, some of them deal with the influence of critical variables on the extraction operation, such as pH, type and quantity of solvent, drying conditions, extraction temperature or maceration type (Reinheimer et al., 2014; Sun et al., 2011).

However, fewer works have addressed the extraction process using first-principles based models to precisely quantify the influence of the aforementioned variables in order to contribute to the process optimization. One important contribution in this field is the work of Garcia-Perez et al. (2010), where the authors proposed a mathematical model to calculate the initial antioxidant capacity of grape stalks, the effective diffusivity of antioxidants in the grape stalk structures and the mass transfer coefficient at the interface for different drying conditions. On the other hand, they did not address the distribution constant and diffusivity of antioxidant at the solvent phase, which are also important variables to describe the mass transfer mechanism. The model proposed by Espinoza-Perez et al. (2007) for caffeine extraction is a more comprehensive one, as it is based on mechanistic principles for the conventional extraction process, in which the mass transfer mechanism at the solvent phase and the distribution constant (determined in previous experiments) were incorporated.

On the other hand, models presented for ultrasound assisted extraction have been limited to describing the kinetics of the extraction by fitting experimental data to the analytical solution of the unsteady-state diffusion equation (D'Alessandro et al., 2014; Ruiz et al., 2011; Tao et al., 2014a).

The contribution here proposed addresses the description of the mechanism of the conventional solvent extraction and ultrasound-assisted extraction of anthocyanins from grape pomace, in order to evaluate and compare the different mass transfer rates. Differences for the mass transfer coefficients values (including diffusion, global mass transfer coefficients and distribution constants) are substantiated from a physical point of view. Therefore, a complete mathematical model to describe the mass transfer mechanism for CSE and UAE methods is here developed using first principles equations through DAEs and semi-empirical correlations, and validated by means of experimental runs. Temperature effect on the anthocyanins transfer kinetics and extraction yield are also studied.

2. Materials and methods

2.1. Raw material and chemicals

Pomace of red grapes (*Vitis vinifera L.*), donated by "Cátedra de Enología II" at "Universidad Nacional de Cuyo", was employed for the development of the extraction experimental runs. Whole pomace was used, whereas seeds and skins were not separated in order to better approximate industrial processing conditions.

An ethanol-water mixture was selected as the extraction mean, since it was reported as one of the best solvent for extraction of polyphenols from grape waste (Librán et al., 2013). Ethanol is the most used solvent in antioxidants extraction, and it is the natural solvent of these compounds in the wine-making process. Other studies have shown that a 50% ethanol solution was the optimal mixture for polyphenols extraction. (Cacace and Mazza, 2003; Do et al., 2014)

136 *2.2. Preparation of grape marc flour*

137 The by-product was prepared according to the conditions reported by Sant'Anna
138 et al. (2012) and Tao et al. (2014a), as they were proven to provide good yields at
139 similar extraction conditions than the ones used in this work. Then, the grape marc
140 samples were dried to about 7.5% moisture content in a dry oven (forced convection
141 laboratory drying equipment) at 60 °C, and afterwards, they were grounded in a
142 domestic mill. The powdered samples were sieved to separate particles passing an
143 ASTM 40 sieve and retained by an ASTM 270 using a Ro-Tap sieve shaker (Tyler, US).
144 Then, a statistical particle diameter, computed according to Vian and Ocón (1952), of
145 0.26 mm was used for the extraction model. The ground samples were sealed and
146 stored at 4 °C in darkness until use.

147

148 *2.3. Determination of initial anthocyanin concentration*

149 The initial content of anthocyanins was determined using the method described
150 by Tao et al. (2014b) with slight modifications. According to preliminary studies, 50%
151 aqueous ethanol was selected as the extraction solvent, as it was observed a high
152 extraction capacity. An amount of 10 g of grape pomace and 400 mL of 50% aqueous
153 ethanol solution were mixed in a 600 mL beaker. Anthocyanins were extracted
154 exhaustively at 45 °C under agitation for 48 h. After that, the liquid extract was
155 separated from the solid by filtration. The residual grape pomace was moved back into
156 the beaker and another 100 mL fresh 50% aqueous ethanol was added. The suspension
157 was treated at 45 °C with agitation for 4 h, followed by filtration. The two filtrates were
158 mixed. The total anthocyanins content in this filtrate was determined using the method
159 explained in Section 2.5 and it was regarded as the initial content of total anthocyanins
160 in the grape pomace, which was determined to be 10.71 mg/g.

161

162 *2.4. Extraction experiments*

163 The extraction experiments were performed with a batch extractor of 0.6 L and a
164 paddle agitator. The extractor was placed in a thermostatic and ultrasonic bath system
165 (TB04, Testlab, Argentina). The ultrasonic system was turned on for UAE, while it was
166 turned off for CSE.

167 In the case of ultrasonic assistance, the sonication was applied in continuous
168 mode at a frequency of 40 kHz and an electric power output of 160 W. Then, the
169 calculated power density of ultrasound dissipated into the medium with an extraction
170 volume of 400 ml was 0.4 W/ml. The ultrasonic energy required for 30 minutes of
171 sonication was 720 J/ml. An acoustic energy density (*AED*) of 36.2 W/l was computed
172 according to Tao et al., (2014a), as the ratio between the consumed power and the total
173 volume of solution used in the experiment.

174 The calculated power density could be considered in the region of low
175 sonication or low intensity treatment, as reported many authors (J. Mason et al., 2011;
176 Karki, 2009; Zhou et al., 2013). This value could be advantageous for energy efficiency
177 studies considering the potentiality of scaling up. Frequency, batch volume and power
178 output could be combined to achieve the desired outcome on a larger scale maintaining
179 a target of low power dissipation. However, a carefully revision of costs should be
180 considered (Karki, 2009). Some efforts of viable scaling up ultrasonic aided extraction
181 have been reported in the literature (Paniwnyk et al., 2009; Vilkhu et al., 2008; Virot et
182 al., 2010; Wang et al., 2015).

183 The temperature in the flask was controlled with a thermometer. The flask
184 containing the mixture was immersed in the bath and fixed in position. The water inside
185 the bath flowed through a circulator system.

In all experiments, for both extraction types, the agitation speed was set at 460 rpm, which gives an agitation velocity of 1.083 m/s when considering an agitator blades diameter of 0.045 m. The initial solid to solvent ratio was fixed to 1:40 (10 g grape marc/sample in 400 mL solvent). Temperature was set at 25, 45 and 65 °C. As solvent, a 50 % vol. ethanol–water mixture was used. In all studied conditions, at specific time intervals (5, 10, 15, 20, 25 and 30 min), 5 ml of the solution were taken for analysis. At the end of each extraction process, the crude extracts were filtered through a Whatman 40 filter. Afterwards, the samples were stored in amber bottles at -4 ºC until the antioxidant activity was measured by spectrophotometry.

After each sample extraction, the extracted volume was not replaced with fresh solvent. Thus, 7.5% of the overall volume is removed in subsequent sampling; since this amount is less than 10% compared to the overall volume, the extraction volume was considered as constant.

2.5. Determination of total anthocyanins

Determination of total anthocyanins in each extracted sample was performed using the method proposed by Di Stefano et al. (1989) and described by Ivanova et al. (2011) by duplicate. Samples were diluted with a solution consisting of ethanol/water/HCl (69/30/1 v/v/v) and the absorbance was measured at 540 nm, in a Jasco Spectrophotometer (7800 UV/Vis). The total anthocyanins content was calculated by means of Eq. (1), as proposed by Di Stefano et al. (1989).

$$C_{a,\gamma} = 16.7\, A_{540nm}\, d \qquad (1)$$

where d is the dilution factor, A_{540nm} is the absorbance at 540 nm, $C_{a,\gamma}$ is the content expressed in mg/L as malvidin-3-glucoside equivalents.

3. Mathematical model

Several possible mass transfer mechanisms have been proposed in order to model the extraction process (Aguilera and Stanley, 1999; Baümler et al., 2011; Cissé et al., 2012; Espinoza-Perez et al., 2007; Garcia-Perez et al., 2010). In this context, the following phenomenological steps are here taken into account:

- Entrance of the solvent into the solid matrix.
- Solvent penetration and diffusion inside the solid matrix.
- Solubilization of the soluble compound.
- Solute transport to the surface of the solid matrix by diffusion.
- Migration of the extracted solute from the external surface into the bulk solution.

3.1. Assumptions

In order to describe the anthocyanin transfer and to study the extraction kinetics, the following hypotheses are used to derive the mathematical model:

- The solid particles are spherical.
- The anthocyanins diffuse to the surface of each sphere according to Fick's second law.
- The anthocyanins in the extracted sample are within the structure of intact cells and as part of disrupted superficial cells. The latter can be produced by physical manipulation and exacerbated by ultrasound.
- The anthocyanins rate of extraction from disrupted cells is comparatively faster than within intact cells. The extraction rate at the first period is assumed to occur by a washing phenomenon.
- Free and bound anthocyanins extraction takes place simultaneously.

- Size, shape and density of the particles do not change during the extraction process. Solid particles are characterized by a given diameter and an initial uniform anthocyanin concentration.
- Temporal variation of the anthocyanins concentration is considered in the radial direction within each particle (1-D model).
- Perfect mixing between solvent and particles.
- Only anthocyanins diffuse from within the solid to the surface. The diffusion coefficient is independent of time.
- Anthocyanins are transferred by convection from the solid surface to the solvent.
- The agitation speed for the ultrasound assisted process is considered approximately 10% higher than for the conventional process to account for the generated shockwaves and high speed jets, and thus the increased mass transfer rate.
- The anthocyanins concentration is homogeneous at the solvent phase (perfect mixing). Solute concentration in the solvent phase is only function of time.
- The anthocyanins concentration at the solid interface is at equilibrium with the anthocyanins concentration at the bulk solvent.
- The volume of the solvent phase is kept constant.
- There are neither chemical reactions nor ultrasonic degradation of anthocyanins during the whole extraction process.

3.2. Equations

Based on the aforementioned assumptions, the internal mass transfer is described by Fick's second law in 1-D and spherical coordinates, applied for the disperse phase of grape pomace flour according to Eq. (2).

$$\frac{(1-\varepsilon)}{D_{a,\beta}}\frac{\partial C_{a,\beta}(r,t)}{\partial t} = (1-\varepsilon)\frac{\partial^2 C_{a,\beta}(r,t)}{\partial r^2} + \frac{2}{r}\frac{(1-\varepsilon)\partial C_{a,\beta}(r,t)}{\partial r}\ ,\ 0 < r < R \qquad (2)$$

where $C_{a,\beta}$ is the anthocyanins concentration inside the particle, and $D_{a,\beta}$ is the diffusivity coefficient of anthocyanins within each particle.

Here, ε is the solvent volume fraction defined by Eq. (3), where V_γ and V_β are the volume of the solvent phase and volume of the solid particle, respectively.

$$\varepsilon = \frac{V_\gamma}{V_\gamma + V_\beta} \quad (3)$$

The initial and boundary conditions are introduced by Eqs. (4-6). Here, Eq. (4) assumes homogeneous initial anthocyanins concentration in the particles; Eq. (5) corresponds to the boundary condition at the center of each sphere where there is no mass transfer; Eq. (6) represents the interfacial anthocyanins flux, where $k_{a,\gamma}$ is the global mass transfer coefficient in the solvent phase, $C_{a,\gamma}$ is the concentration in the bulk solvent and $C_{a,\gamma,i}$ is the concentration of anthocyanins at the solid-solvent interphase.

$$C_{a,\beta}(r,t) = C_{a0,\beta}\,, 0 \le r \le R\,, t = 0 \quad (4)$$

$$\frac{\partial C_{a,\beta}(r,t)}{\partial r} = 0\,, r = 0\,, t > 0 \quad (5)$$

$$-D_{a,\gamma}\frac{\partial C_{a,\beta}(r,t)}{\partial r} = k_{a,\gamma}\left(C_{a,\gamma,i}\,(t) - C_{a,\gamma}(t)\right), r = R\,, t > 0 \quad (6)$$

A typical simplification, extensively used in chemical engineering mass transfer operations including solid–liquid extraction (Geankoplis, 1993), is the representation of the mass transfer in both phases with macroscopic models. The macroscopic mass transfer into the solvent phase is described by Eq. (7), while Eq. (8) represents the macroscopic mass transfer in the particles, and Eq. (9) gives the non-accumulation in the interface.

$$\varepsilon\frac{dC_{a,\gamma}(t)}{dt} = k_{a,\gamma}\ s\left(C_{a,\gamma i}(t) - C_{a,\gamma}(t)\right), 0 < t < t_f \quad (7)$$

$$(1-\varepsilon)\frac{d\langle C_{a,\beta}\rangle(t)}{dt} = k_{a,\beta}\,s\left(C_{a,\beta,i}(t) - \langle C_{a,\beta}\rangle(t)\right), 0 < t < t_f \quad (8)$$

$$k_{a,\gamma}\left(C_{a,\gamma i}(t)-C_{a,\gamma}(t)\right)=-k_{a,\beta}\left(C_{a,\beta,i}(t)-\langle C_{a,\beta}\rangle(t)\right),0<t<t_f \quad (9)$$

Afterwards, Eqs. (7-9) can be reduced to Eq. (10), thus obtaining a system which is consistent with respect to the mass balances.

$$(1-\varepsilon)\frac{d\langle C_{a,\beta}\rangle(t)}{dt}=-\varepsilon\frac{dC_{a,\gamma}(t)}{dt},\ 0<t<t_f \quad (10)$$

Here, s is the specific surface for mass transfer for spherical particles, as defined by Eq. (11).

$$s=\frac{6}{2R} \quad (11)$$

The equilibrium at the interface of the anthocyanins concentration under the assumption of diluted solution, is expressed by means of Eq. (12), where K is the distribution constant.

$$C_{a,\gamma i}(t)=K\,C_{a,\beta,i}(t)\,,r=R\,,t>0 \quad (12)$$

Extraction yield (Y) is a measure of the solvent efficiency to extract specific components from the original material, according to Eq. (13), and is calculated as the ratio of the amount of anthocyanins extracted and the initial amount of anthocyanins present in the grape pomace flour.

$$Y(t)=\frac{m_{a,\gamma}(t)}{m_{a0,\beta}}\,100=\frac{C_{a,\gamma}(t)\,V_\gamma}{C_{a0,\beta}\,V_\beta}\,100\,,\mathrm{t}>0 \quad (13)$$

The estimation of the average anthocyanins concentration at each instant of time in the solid spheres is obtained by integrating local concentrations over volume. Specifically, the average anthocyanins concentration in the phase β is expressed as stated in Eq. (14), which can be solved by means of Simpson's rule.

$$\langle C_{a,\beta}\rangle(t)=\frac{\int_0^V C_{a,\beta}(r,t)dV}{\int_0^V dV},\mathrm{t}\geq 0 \quad (14)$$

The anthocyanins mass balance into the solid particle and the solvent is given as: [Initial mass of anthocyanins in grape pomace flour] = [Mass of anthocyanins in

disperse solid phase] + [Mass of anthocyanins in solvent phase]. Therefore, Eqs. (15-16) represent the mass balances at the initial time and at equilibrium.

$$C_{a0,\beta}\, V_\beta = \langle C_{a,\beta} \rangle_{t=t_0}\, V_\beta \quad (15)$$

$$C_{a0,\beta}\, V_\beta = \langle C_{a,\beta} \rangle_{t=t_f}\, V_\beta + C_{a,\gamma}{}_{t=t_f}\, V_\gamma \quad (16)$$

3.4. Parameters

The main model parameters can be classified into the following categories:

- Operating conditions used for extraction experiences: temperature and extraction time, solvent volume fraction, agitation velocity, particle diameter, and acoustic energy density for UAE method.
- Physical properties: density, viscosity and molecular weight of solvent, molar volume of solute at its boiling point.
- Mass transfer coefficients: internal and external mass transfer coefficients.

Table 1 lists the main model input data related to experimental results and physicochemical properties obtained by means of commercial software of from the literature.

Also note that it is also hereafter proposed to implement, where available and valid, correlations reported in the literature to predict the mass transfer coefficients. This strategy also facilitates the resolution of the non-linear mathematical model, as the degrees of freedom are reduced (if the degrees of freedom are high, the optimal solution could be inconsistent from the physics point of view).

3.4.1. Anthocyanin diffusivity coefficient within the particles

Tao et al. (2014a) developed an empirical correlation based on the Fick's second law to estimate the effective diffusion coefficient $D_{a,\beta}$ of phenolic compounds from

grape marc considering the effects of the acoustic energy density *(AED)* and the extraction temperature, using ethanol solution of 50%. The correlations developed for total phenolic compounds are applied to calculate the anthocyanin diffusivity coefficient for the ultrasound assisted extraction. Two correlations are proposed by Tao et al. (2014a) considering that the mechanism of the extraction process is formed by two stages: a first step of washing (dissolution of anthocyanins near the particle surface), in which a rapid increase of extraction yield is evidenced, according to Eq. (17); and a second stage in which the extraction process is slower (diffusion from the solid particles to the liquid extract), according to Eq. (18). In addition, Tao et al. (2014a) found experimentally that the transition from the washing stage to the slow extraction stage takes place for a fraction of total phenolics released in the range of 85-93%.

$$D_{a,\beta-fast} = 8.913x10^{-30}\ (AED)^{0.6927}\ (T + 273.15)^{7.087} \quad (17)$$

$$D_{a,\beta-slow} = 5.525x10^{-19}\ (AED)^{0.1459}\ (T + 273.15)^{2.701} \quad (18)$$

No works reporting correlations for the estimation of the diffusion coefficient within the particles for the CSE method have been found. Note that in the model, the mechanism of the conventional extraction process is also considered as occurring in two stages (washing and slow extraction). Then, these coefficients are kept as optimization variables in the mathematical model.

3.4.2. Anthocyanin diffusivity coefficient at the solvent phase

For conventional solvent extraction, the Wilke and Chang (1955) correlation was used to estimate the anthocyanins diffusion coefficient at the solvent phase $D_{a,\gamma}$, which is recommended for biological solutes, as given by Eq. (19).

$$D_{a,\gamma} = 1.173E10^{-16}\left(\varphi\ MW_{\gamma}\right)^{0.5}\ \frac{T+273.15}{\mu_{\gamma}\ V_{m,a}^{0.6}} \quad (19)$$

No works reporting correlations for the estimation of the diffusion coefficient at the solvent phase for the UAE method have been found. Then, these coefficients are kept as optimization variables in the mathematical model.

3.4.3. Global mass transfer coefficient

The global mass transfer coefficient $k_{a,\gamma}$ was calculated using the correlation proposed by Geankoplis (1993) for fixed beds and also valid for fluidized beds of spheres in the Reynolds number range of (2–2,000), according to Eq. (20), in conjunction with Eqs. (21-23).

$$Sh = 2 + 0.95\ (Re)^{0.5}\ (Sc)^{1/3} \quad (20)$$

$$k_{a,\gamma} = \frac{Sh\ D_{a,\gamma}}{2\ R} \quad (21)$$

$$Sc = \frac{\mu_\gamma}{D_{a,\gamma}\ \rho_\gamma} \quad (22)$$

$$Re = \frac{2\ R\ \rho_\gamma\ v}{\mu_\gamma} \quad (23)$$

3.5. Resolution strategy

Eqs. (2, 5-7) were discretized using the central finite difference method (CFDM) and the implicit method. This scheme, which has first-order accuracy in time and second-order accuracy in space, is unconditionally stable and convergent. Eqs. (24-25) define the radial and temporal variations, respectively, with M = 6 and N = 6.

$$\delta = \frac{R}{M} \quad (24)$$

$$\Delta t = \frac{t_f}{N} \quad (25)$$

Eq. (26) computes the approximation of Eq. (2) for internal nodes.

$$\frac{(1-\varepsilon)\left(C_{a,\beta}(r,t+1)-C_{a,\beta}(r,t)\right)}{D_{a,\gamma}\,\Delta t} = (1-\varepsilon)\left(\frac{C_{a,\beta}(r-1,t+1)-2\,C_{a,\beta}(r,t+1)+C_{a,\beta}(r+1,t+1)}{\delta^2} + \frac{C_{a,\beta}(r+1,t+1)-C_{a,\beta}(r-1,t+1)}{2\delta}\right), 0 < r < R; 0 < t < t_f \quad (26)$$

Eqs. (27-28) are the constraints related to the discretization of Eqs. (5-6), which are the boundary conditions at the center and surface of each solid particle, respectively.

$$\frac{-3\,C_{a,\beta}(r,t)+4\,C_{a,\beta}(r+1,t)-C_{a,\beta}(r+2,t)}{2\,\delta} = 0\,, r = 0\,, t > 0 \quad (27)$$

$$-D_{a,\gamma}\,\frac{C_{a,\beta}(r-2,t)-4\,C_{a,\beta}(r-1,t)+3\,C_{a,\beta}(r,t)}{2\,\delta} = k_{a,\gamma}\left(C_{a,\gamma,i}(t) - C_{a,\gamma}(t)\right)\,, r = R\,, t > 0 \quad (28)$$

Eq. (29) computes the approximation of Eq. (10).

$$(1-\varepsilon)\,\frac{\langle C_{a,\beta}\rangle(t+1)-\langle C_{a,\beta}\rangle(t)}{\Delta t} = -\varepsilon\,\frac{C_{a,\gamma}(t+1)-C_{a,\gamma}(t)}{\Delta t}, 0 < t < t_f \quad (29)$$

Therefore, the proposed mathematical model for conventional and ultrasound-assisted techniques for extraction of anthocyanins from grape pomace is summarized in Figure 1. Here, equations which are used for representing only one or both techniques, CSE and UAE, can be easily identified.

In order to obtain the optimal values of the practical interest variables, the root-mean-square error (RMSE) is minimized, as it represents the sum of the differences between the experimental data points ant the corresponding values predicted by the model. The proposed non-linear programming model was implemented in GAMS (General Algebraic Modeling System) and solved using CONOPT (Drud, 1996), an algorithm based on the reduced gradient method. The resulting model involves 452 variables and 430 constraints.

401 **4. Results and discussion**

402 *4.1. Kinetics of extraction*

403 Figure 2 plots the experimental data points and the predicted evolution of the
404 anthocyanins concentration at the solvent phase ($C_{a,Y}$) during the CSE and UAE
405 experiences. It is observed that, for both methods and all temperatures, anthocyanin
406 concentration increased asymptotically tending to an equilibrium concentration.

407 As observed in Figure 2, the kinetic behavior between CSE and UAE exhibits
408 different trends for the washing stage, where the anthocyanins concentration in the
409 solvent phase grows quickly. The washing stage for UAE is faster than for CSE at the
410 same temperature and solvent ratio.

411 The equilibrium concentration for UAE is obtained between 300 and 600
412 seconds before than for CSE. The enhancement in the extraction rate for UAE obtained
413 by the disruption of cell walls are in accordance with the results reported by
414 Balachandran et al. (2006); Hemwimol et al. (2006); Ruiz et al. (2011); Veličković et al.
415 (2006) and Zhao et al. (2007).

416 As can be seen in Figure 2, the extraction kinetic curves are improved by the
417 extraction temperature over the examined range. At extraction temperatures of 25, 45,
418 and 65 °C, the maximum anthocyanins concentration obtained for CSE at 1800 seconds
419 are 0.373, 0.453 and 0.475 mg/mL, respectively. Meanwhile, the maximum
420 anthocyanins concentration obtained for UAE at 1800 seconds are 0.386, 0.475 and
421 0.479 mg/mL at the same temperatures. When compared, about 80% anthocyanins were
422 extracted in the first 600 seconds for CSE, while 90% of anthocyanins were recovered
423 for UAE in the same time. These values were close to the ones reported by Garcia-Perez
424 et al. (2010) for the antioxidant extraction from grape pomace using ethanol as solvent.

Equilibrium concentration is reached in the early minutes of the extraction. After 1800 seconds, the extraction yield increased only by 1–5% and 0.7-1% for CSE and UAE, respectively. According to the obtained experimental results, it is also observed that the extraction yield of anthocyanins increases as temperature does.

In order to evaluate the effect of ultrasound on the extraction kinetics, Eq. (30) is used, where $Y|_{UAE}$ is the extraction yield with ultrasonic assistance and $Y|_{CSE}$ is the extraction yield without irradiation.

$$\text{Effect of UAE}(t) = \frac{(Y(t)|_{UAE} - Y(t)|_{CSE})}{Y(t)|_{CSE}} 100 \quad (30)$$

Figure 3 compares the time evolution of the ultrasound effect on total anthocyanins extraction yield at the three experimental temperatures. It can be observed that the ultrasonic effect enhances the mass transfer rate at the beginning of the extraction process, i.e. the washing stage. In fact, ultrasound waves and the cavitation effect they produce can alter biological materials and their physical and chemical properties, facilitating the release of extractable compounds and enhancing mass transport by disrupting cell walls (Chemat et al., 2011). It can be assumed that the cavitation process incited by ultrasound provokes cells swelling, solvent uptake, pores enlargement, and therefore a diffusivity increment across the cell walls. A possible disruption of plant cell walls or small positive effect on extraction due to local ultrasound heating of the vegetal source could also be noticed (D'Alessandro et al., 2014).

It was observed that the effect of ultrasound was always higher in the beginning of the extraction processes and it decreased considerably with the extraction time, while it had a less noticeable effect in the obtained equilibrium values for the total anthocyanins concentration in the solvent.

450 *4.2. Analysis of the mass transfer properties*

451 Table 2 summarizes the values of the mass transfer coefficients and the
452 goodness of fit of the model to the obtained experimental data.

453 First of all, it can be observed in Table 2 that the accuracy of the model to
454 predict the anthocyanin concentration evolution at the solvent phase is satisfactory for
455 both extraction processes, CSE and UAE, according to the reported statistical
456 parameters. The goodness of fit may be observed in the values close to 1 of the
457 determination coefficient (R^2) and small root mean square error (RMSE) values, thus
458 indicating a good agreement between experimental and predicted values.

459 In most cases in the food processing industry (Cissé et al., 2012; Tao et al.,
460 2014a), the solubility and diffusion coefficient of the material which is being extracted
461 will increase with temperature, resulting in a higher rate of extraction. Nevertheless, the
462 processing temperature cannot be increased indefinitely, because bioactive compounds
463 are relatively thermo-labile, being susceptible to degradation at high temperatures
464 (Pingret et al., 2013).

465 Accordingly, it was here found that the effective diffusion coefficient of
466 anthocyanins $D_{a,\beta}$ at both CSE and UAE experiences increased with temperature, which
467 may be caused by an increment of the internal energy of the molecules and thus their
468 mobility, and a reduction of the dynamic viscosity coefficient.

469 In the model here presented, the diffusion process is considered as a fast
470 diffusion stage (washing process) followed by a slow transfer rate (slow extraction).
471 Following the proposal by Tao et al. (2014a), the transition was here determined to
472 occur at an anthocyanin extracted fraction of around 84% for CSE and around 90% for
473 UAE. It is also observed that the diffusivity coefficients for CSE (computed by the

model) are lower than for UAE (estimated through empirical correlations) in both stages, although the difference is larger at the washing stage.

The obtained values for the diffusion coefficients are similar to the ones reported in the literature for grape by-products. For CSE, the value of the diffusivity coefficients reported in Table 2 are of the same order of magnitude of those obtained by Garcia-Perez et al. (2010) at an extraction temperature of 60°C and Bucić-Kojić et al. (2013) at extraction temperatures in the range of 25 to 80°C. For UAE, the internal diffusion coefficients obtained using the empirical correlation proposed by Tao et al. (2014a) are similar to those obtained in the studies of ultrasound-assisted extractions of antioxidants from pomegranate peels and oil from pomegranate seeds reported by Goula (2013) and Pan et al. (2011), respectively.

The values obtained for the diffusivity of the anthocyanins at the solvent phase $D_{a,\gamma}$, the global mass transfer coefficient in the solvent phase $k_{a,\gamma}$, and the distribution constant K, all follow similar increasing trends as the temperature does.

The global mass transfer coefficient is function of the agitation speed, which remains constant for each extraction method; while due to the increment in the agitation speed and the solvent diffusivity value for the UAE experiences, $k_{a,\gamma}$ is higher for the same temperature than for the CSE ones.

4.3. Prediction and confidence bands

Figure 4 presents the confidence band (CB) and prediction band (PB) for the anthocyanin concentration at the solvent phase against time for the CSE and UAE experiences, respectively, at an operating temperature of 45 ºC. It is noted that similar trends were observed when working at 25 and 65 ºC.

The PB is the region where 95% of the experimental data points are expected to be, whereas it is here observed that all obtained observations fall within. Likewise, the CB is the region where 95% of the regression lines are expected to be, and contain more than 50% of the experimental values for all the experiences here reported. Both obtained CB and PB are well adjusted to the experimental data points, therefore increasing the confidence on the values predicted for the model parameters.

Normal probability plots of residuals are also presented in Figure 5 for the CSE and UAE experimental runs at 45 ºC, respectively. As the data points are equally distributed above and below the line, it is verified that they are normally distributed and no unwanted trends or correlations among the data points exist (skewness, presence of an undefined variable, outliers, among others).

4.4. Sensitivity analysis

In this section, parameters from empirical correlations and variables obtained through the proposed model are varied between -30% and 30%, in order to analyze their impact in the extraction yield. Figure 6 presents spider diagrams for CSE and UAE at 65 ºC for the fast and slow extraction periods. It is noted that similar trends were observed when working at 25 and 45 ºC.

As can be appreciated in all figures, the internal diffusivity coefficient exerts the larger impact over the extraction yield, as it is the controlling process for the conventional and ultrasound assisted extraction of bio compounds. Therefore, the rest of the mass transfer parameters (diffusivity coefficients at solvent phase as well as global mass transfer coefficients) have little effect on the extraction yield.

The results here obtained are in agreement with the literature (Bucić-Kojić et al., 2013; Tao et al., 2014a), where it is expected that the internal diffusion is the controlling

523 step of the process, in which higher extraction rates are obtained for higher diffusion
524 coefficients.
525
526 *4.5. Performance of the extraction*
527 The proposed mathematical model for the extraction of anthocyanins from grape
528 pomace could also be used to achieve predictions for the system behavior when working
529 at different operative temperatures (or eventually, other practical interest parameters).
530 Figure 7 presents the expected performance of the system for 30, 35, 40, 50, 55 and 60
531 ºC, which are intermediate to the ones used in the experimental runs.
532 For the new temperature values, it should be noted that the diffusivity coefficient
533 within particles for UAE and the diffusivity coefficient at solvent for CSE were
534 computed from the empirical correlations reported in section 3.4; while the rest of the
535 mass transport properties were linearly interpolated from the values reported in Table 2.
536 It is then reaffirmed that temperature has a positive effect on extraction
537 efficiencies; although caution should be exercised since high temperatures promote the
538 oxidative reaction of phenolic compounds, which result in higher degradation rates.
539 Figure 8 allows estimating the extraction time necessary to achieve a value of
540 the extraction yield of 50, 75 and 90%, when operating at temperatures in the range of
541 25-65 ºC. For both techniques (CSE and UAE), it is observed that the same
542 anthocyanins yield can be obtained at lower extraction times as the temperature is
543 increased.
544 Moreover, the effect of temperature becomes more noticeable for larger values
545 of the extraction yield; while a 90% recovery may only be achieved when working
546 above 55 ºC for CSE and above 50 ºC for UAE. As expected, the required operating
547 time for reaching a given extraction yield is drastically reduced by the use of ultrasound

548 assistance; while for a given operative temperature, a higher yield is achieved for a
549 longer extraction time.

550 The increment of extraction yield with temperature under CSE may be explained
551 in the accelerated softening and swelling of materials and the increased solubility and
552 diffusivity of anthocyanins.

553 In the case of UAE, the variation of extraction yield with temperature may be
554 attributed to the combination of the cavitation and thermal effects. At lower
555 temperatures, vapor pressure is low and ultrasound produces few cavitation bubbles.
556 However, bubbles explode with a relatively large force, which enhances cell tissue
557 disruption during extraction. Rising extraction temperature can result in an increase of
558 vapor pressure and decrease of surface tension, thus decreasing energies released during
559 the collapse of cavitation bubbles. Bubbles may easily collapse at higher temperatures
560 thus reducing the enhancement of the mass transfer intensity. At higher temperatures,
561 ultrasonic cavitation can be altered and the phenolic compounds may be oxidized.

562

563 **5. Conclusions**

564 In this work, experimental runs for the conventional and ultrasound-assisted
565 extraction of anthocyanins from grape pomace are reported and thoroughly analyzed.
566 Then, a complete mathematical model to describe the mass transfer mechanism for both
567 methods is developed using first principles equations through DAEs and semi-empirical
568 correlations.

569 Several statistical parameters show that the proposed model satisfactorily
570 predicts the anthocyanin concentration evolution at the solvent phase for both extraction
571 processes, CSE and UAE, while computing several mass transport coefficients,

including the diffusivities within the particle and at the solvent phase, the global mass transfer coefficient in the solvent phase, and the distribution constant.

Afterwards, the expected performance of the extraction for different operative conditions is predicted, thus providing useful information for designing, optimizing and scaling up of the conventional and ultrasound-assisted recovery of anthocyanins in the food processing industry.

Further analysis considering other important process variables such as agitation speed and solute-solvent ratio will be developed in future works.

Acknowledgments

The authors kindly acknowledge the financial support of the Universidad Tecnológica Nacional (UTN) and the Consejo Nacional de Investigaciones Científicas y Técnicas (CONICET) of Argentina.

References

Aguilera, J.M., Stanley, D.W., 1999. Microstructural Principles of Food Processing and Engineering. Springer Science & Business Media.

Balachandran, S., Kentish, S., Mawson, R., Ashokkumar, M., 2006. Ultrasonic enhancement of the supercritical extraction from ginger. Ultrason. Sonochem. 13, 471–479. doi:10.1016/j.ultsonch.2005.11.006

Balasundram, N., Sundram, K., Samman, S., 2006. Phenolic compounds in plants and agri-industrial by-products: Antioxidant activity, occurrence, and potential uses. Food Chem. 99, 191–203. doi:10.1016/j.foodchem.2005.07.042

Banga, J.R., Balsa-Canto, E., Moles, C.G., Alonso, A.A., 2003. Improving food processing using modern optimization methods. Trends Food Sci. Technol. 14, 131–144. doi:10.1016/S0924-2244(03)00048-7

Baümler, E.R., Carelli, A.A., Crapiste, G.H., Carrín, M.E., 2011. Solvent extraction modeling of vegetable oil and its minor compounds. J. Food Eng. 107, 186–194. doi:10.1016/j.jfoodeng.2011.06.025

Both, S., Chemat, F., Strube, J., 2014. Extraction of polyphenols from black tea – Conventional and ultrasound assisted extraction. Ultrason. Sonochem. 21, 1030–1034. doi:10.1016/j.ultsonch.2013.11.005

Bucić-Kojić, A., Sovová, H., Planinić, M., Tomas, S., 2013. Temperature-dependent kinetics of grape seed phenolic compounds extraction: experiment and model. Food Chem. 136, 1136–1140. doi:10.1016/j.foodchem.2012.09.087

Cacace, J. e., Mazza, G., 2003. Optimization of Extraction of Anthocyanins from Black Currants with Aqueous Ethanol. J. Food Sci. 68, 240–248. doi:10.1111/j.1365-2621.2003.tb14146.x

Chemat, F., Zill-e-Huma, N., Khan, M.K., 2011. Applications of ultrasound in food technology: Processing, preservation and extraction. Ultrason. Sonochem. 18, 813–835. doi:10.1016/j.ultsonch.2010.11.023

Cheng, Z., Zhang, Y., Song, H., Zhou, H., Zhong, F., Hu, H., Feng, Y., 2016. Extraction optimization, characterization and antioxidant activity of polysaccharide from Gentiana scabra bge. Int. J. Biol. Macromol. 93, Part A, 369–380. doi:10.1016/j.ijbiomac.2016.08.059.

Cissé, M., Bohuon, P., Sambe, F., Kane, C., Sakho, M., Dornier, M., 2012. Aqueous extraction of anthocyanins from Hibiscus sabdariffa: Experimental kinetics and modeling. J. Food Eng. 109, 16–21. doi:10.1016/j.jfoodeng.2011.10.012.

Da Porto, C., Porretto, E., Decorti, D., 2013. Comparison of ultrasound-assisted extraction with conventional extraction methods of oil and polyphenols from grape (Vitis vinifera L.) seeds. Ultrason. Sonochem. 20, 1076–1080. doi:10.1016/j.ultsonch.2012.12.002.

D'Alessandro, L.G., Dimitrov, K., Vauchel, P., Nikov, I., 2014. Kinetics of ultrasound assisted extraction of anthocyanins from Aronia melanocarpa (black chokeberry) wastes. Chem. Eng. Res. Des. 92, 1818–1826. doi:10.1016/j.cherd.2013.11.020.

Di Stefano, R., Cravero, M.C., Gentilini, N., 1989. Metodi per lo studio dei polifenoli dei vini. L'Enotecnico 83–89.

Do, Q.D., Angkawijaya, A.E., Tran-Nguyen, P.L., Huynh, L.H., Soetaredjo, F.E., Ismadji, S., Ju, Y.-H., 2014. Effect of extraction solvent on total phenol content, total flavonoid content, and antioxidant activity of Limnophila aromatica. J. Food Drug Anal. 22, 296–302. doi:10.1016/j.jfda.2013.11.001.

Drud, A.S., 1996. CONOPT, ARKI Consulting and Development A/S, Bagsvaerd, Denmark. See also: http://www.gams.com/docs/document.htm.

Espinoza-Perez, J.D., Vargas, A., Robles-Olvera, V.J., Rodriguez-Jimenes, G.C., Garcia-Alvarado, M.A., 2007. Mathematical modeling of caffeine kinetic during solid–liquid extraction of coffee beans. J. Food Eng. 81, 72–78. doi:10.1016/j.jfoodeng.2006.10.011.

Garcia-Perez, J.V., García-Alvarado, M.A., Carcel, J.A., Mulet, A., 2010. Extraction kinetics modeling of antioxidants from grape stalk (Vitis vinifera var. Bobal): Influence of drying conditions. J. Food Eng. 101, 49–58. doi:10.1016/j.jfoodeng.2010.06.008.

Geankoplis, C.J., 1993. Transport Processes and Unit Operations. PTR Prentice Hall.

Goula, A.M., 2013. Ultrasound-assisted extraction of pomegranate seed oil – Kinetic modeling. ResearchGate 117, 492–498. doi:10.1016/j.jfoodeng.2012.10.009.

He, B., Zhang, L.-L., Yue, X.-Y., Liang, J., Jiang, J., Gao, X.-L., Yue, P.-X., 2016. Optimization of Ultrasound-Assisted Extraction of phenolic compounds and anthocyanins from blueberry (Vaccinium ashei) wine pomace. Food Chem. 204, 70–76. doi:10.1016/j.foodchem.2016.02.094.

Hemwimol, S., Pavasant, P., Shotipruk, A., 2006. Ultrasound-assisted extraction of anthraquinones from roots of Morinda citrifolia. Ultrason. Sonochem. 13, 543–548. doi:10.1016/j.ultsonch.2005.09.009.

Ivanova, V., Dörnyei, Á., Márk, L., Vojnoski, B., Stafilov, T., Stefova, M., Kilár, F., 2011. Polyphenolic content of Vranec wines produced by different vinification conditions. Food Chem. 124, 316–325. doi:10.1016/j.foodchem.2010.06.039.

J. Mason, T., Chemat, F., Vinatoru, M., 2011. The Extraction of Natural Products using Ultrasound or Microwaves. Curr. Org. Chem. 15, 237–247. doi:10.2174/138527211793979871.

Karki, B., 2009. Use of high-power ultrasound during soy protein production and study of its effect on functional properties of soy protein isolate.

Librán, C.M., Mayor, L., Garcia-Castello, E.M., Vidal-Brotons, D., 2013. Polyphenol extraction from grape wastes: Solvent and pH effect. Agric. Sci. 4, 56. doi:10.4236/as.2013.49B010.

Meneses, M.A., Caputo, G., Scognamiglio, M., Reverchon, E., Adami, R., 2015. Antioxidant phenolic compounds recovery from Mangifera indica L. by-products by supercritical antisolvent extraction. J. Food Eng. 163, 45–53. doi:10.1016/j.jfoodeng.2015.04.025.

Monrad, J.K., Howard, L.R., King, J.W., Srinivas, K., Mauromoustakos, A., 2010. Subcritical Solvent Extraction of Anthocyanins from Dried Red Grape Pomace. J. Agric. Food Chem. 58, 2862–2868. doi:10.1021/jf904087n.

Pan, Z., Qu, W., Ma, H., Atungulu, G.G., McHugh, T.H., 2011. Continuous and pulsed ultrasound-assisted extractions of antioxidants from pomegranate peel. Ultrason. Sonochem. 18, 1249–1257. doi:10.1016/j.ultsonch.2011.01.005.

Paniwnyk, L., Cai, H., Albu, S., Mason, T.J., Cole, R., 2009. The enhancement and scale up of the extraction of anti-oxidants from Rosmarinus officinalis using ultrasound. Ultrason. Sonochem. 16, 287–292. doi:10.1016/j.ultsonch.2008.06.007.

Pingret, D., Fabiano-Tixier, A.-S., Chemat, F., 2013. Degradation during application of ultrasound in food processing: A review. Food Control 31, 593–606. doi:10.1016/j.foodcont.2012.11.039.

Qu, W., Pan, Z., Ma, H., 2010. Extraction modeling and activities of antioxidants from pomegranate marc. J. Food Eng. 99, 16–23. doi:10.1016/j.jfoodeng.2010.01.020.

Reinheimer, M.A., Medina, J.R., Scenna, N.J., Mussati, S.F., Freyre, M., Pérez, G.A., 2014. Mathematical modeling and simulation of soluble protein extraction during leaching process in surimi elaboration. J. Food Eng. 120, 167–174. doi:10.1016/j.jfoodeng.2013.07.030.

Ruiz, R.S., Martínez, C., Vizcarra, M.G., 2011. Modeling conventional and ultrasound-assisted extraction of oil-containing materials. Rev. Mex. Ing. Quím. 10, 387–399.

Sant'Anna, V., Brandelli, A., Marczak, L.D.F., Tessaro, I.C., 2012. Kinetic modeling of total polyphenol extraction from grape marc and characterization of the extracts. Sep. Purif. Technol. 100, 82–87. doi:10.1016/j.seppur.2012.09.004.

Spigno, G., De Faveri, D.M., 2007. Antioxidants from grape stalks and marc: Influence of extraction procedure on yield, purity and antioxidant power of the extracts. J. Food Eng. 78, 793–801. doi:10.1016/j.jfoodeng.2005.11.020.

Stevenson, D.E., Hurst, R.D., 2007. Polyphenolic phytochemicals-just antioxidants or much more? Cell. Mol. Life Sci. CMLS 64, 2900–2916. doi:10.1007/s00018-007-7237-1.

Sun, Y., Liu, D., Chen, J., Ye, X., Yu, D., 2011. Effects of different factors of ultrasound treatment on the extraction yield of the all-trans-β-carotene from citrus peels. Ultrason. Sonochem. 18, 243–249. doi:10.1016/j.ultsonch.2010.05.014.

703 Tao, Y., Zhang, Z., Sun, D.-W., 2014a. Kinetic modeling of ultrasound-assisted
704 extraction of phenolic compounds from grape marc: Influence of acoustic energy
705 density and temperature. Ultrason. Sonochem. 21, 1461–1469.
706 doi:10.1016/j.ultsonch.2014.01.029.
707 Tao, Y., Zhang, Z., Sun, D.-W., 2014b. Experimental and modeling studies of
708 ultrasound-assisted release of phenolics from oak chips into model wine.
709 Ultrason. Sonochem. 21, 1839–1848. doi:10.1016/j.ultsonch.2014.03.016.
710 Valdés, A., Vidal, L., Beltrán, A., Canals, A., Garrigós, M.C., 2015. Microwave-
711 assisted extraction of phenolic compounds from almond skin byproducts (prunus
712 amygdalus): A multivariate analysis approach. J. Agric. Food Chem. 63, 5395–
713 5402.
714 Veličković, D.T., Milenović, D.M., Ristić, M.S., Veljković, V.B., 2006. Kinetics of
715 ultrasonic extraction of extractive substances from garden (Salvia officinalis L.)
716 and glutinous (Salvia glutinosa L.) sage. Ultrason. Sonochem. 13, 150–156.
717 doi:10.1016/j.ultsonch.2005.02.002
718 Vian, A., Ocón, T., 1952. Elementos de Ingeniería Química. Colección Ciencia y
719 Técnica. Aguilar.
720 Vilkhu, K., Mawson, R., Simons, L., Bates, D., 2008. Applications and opportunities for
721 ultrasound assisted extraction in the food industry — A review. Innov. Food Sci.
722 Emerg. Technol., Food Innovation: Emerging Science, Technologies and
723 Applications (FIESTA) Conference 9, 161–169. doi:10.1016/j.ifset.2007.04.014
724 Virot, M., Tomao, V., Le Bourvellec, C., Renard, C.M.C.G., Chemat, F., 2010. Towards
725 the industrial production of antioxidants from food processing by-products with
726 ultrasound-assisted extraction. Ultrason. Sonochem., Sonochemistry: Scale up
727 and industrial development 17, 1066–1074. doi:10.1016/j.ultsonch.2009.10.015
728 Wang, W., Ma, X., Xu, Y., Cao, Y., Jiang, Z., Ding, T., Ye, X., Liu, D., 2015.
729 Ultrasound-assisted heating extraction of pectin from grapefruit peel:
730 Optimization and comparison with the conventional method. Food Chem. 178,
731 106–114. doi:10.1016/j.foodchem.2015.01.080.
732 Wilke, C.R., Chang, P., 1955. A. Z. Ch. E. J. 1, 264.
733 Yim, H.S., Chye, F.Y., Koo, S.M., Matanjun, P., How, S.E., Ho, C.W., 2012.
734 Optimization of extraction time and temperature for antioxidant activity of
735 edible wild mushroom, Pleurotus porrigens. Food Bioprod. Process. 90, 235–
736 242. doi:10.1016/j.fbp.2011.04.001.
737 Zhao, S., Kwok, K.-C., Liang, H., 2007. Investigation on ultrasound assisted extraction
738 of saikosaponins from Radix Bupleuri. Sep. Purif. Technol. 55, 307–312.
739 doi:10.1016/j.seppur.2006.12.002.
740 Zhou, C., Ma, H., Yu, X., Liu, B., Yagoub, A.E.-G.A., Pan, Z., 2013. Pretreatment of
741 defatted wheat germ proteins (by-products of flour mill industry) using
742 ultrasonic horn and bath reactors: Effect on structure and preparation of ACE-
743 inhibitory peptides. Ultrason. Sonochem. 20, 1390–1400.
744 doi:10.1016/j.ultsonch.2013.04.005.
745

Table 1. Model input data

Shape variable or property		Value	Source
R (m)		$1.300\text{x}10^{-4}$	Experimental result
$C_{a0,\beta}$ (kg/m^3)		10.71	Experimental result
$v\|_{CSE}$ (m/s)		1.083	Experimental result
$v\|_{UAE}$ (m/s)		1.200	Experimental result
a (m^2/m^3)		$2.307\text{x}10^{4}$	Experimental result
ε (-)		0.957	Experimental result
AED (W/m^3)		$36.158\text{x}10^{3}$	Experimental result
MW_γ (kg/kmol)		32.034	HYSYS (Hysys, Operations Guide., 2005)
μ_γ (kg/ms^2)	T=25°C	$1.011\text{x}10^{-3}$	HYSYS (Hysys, Operations Guide., 2005)
	T=45°C	$0.715\text{x}10^{-3}$	
	T=65°C	$0.527\text{x}10^{-3}$	
ρ_γ (kg/m^3)	T=25°C	940.2	HYSYS (Hysys, Operations Guide., 2005)
	T=45°C	923.1	
	T=65°C	905.4	
$V_{m,a}$ (m^3/kmol)		0.522	(Geankoplis, 1993)
φ (-)		2.050	(Geankoplis, 1993)

Table

Table 2. Practical interest parameters obtained through the proposed model.

Parameter	**CSE**			**UAE**		
	T=25°C	T=45°C	T=65°C	T=25°C	T=45°C	T=65°C
$D_{a,\beta-fast}$ (m^2/s)	8.586×10^{-12}	9.226×10^{-12}	9.784×10^{-12}	3.678×10^{-11}	5.828×10^{-11}	8.978×10^{-11}
$D_{a,\beta-slow}$ (m^2/s)	7.977×10^{-12}	9.225×10^{-12}	9.784×10^{-12}	4.499×10^{-12}	5.361×10^{-12}	6.321×10^{-12}
$D_{a,\gamma}$ (m^2/s)	4.142×10^{-10}	6.250×10^{-10}	9.016×10^{-10}	4.120×10^{-8}	4.855×10^{-8}	5.601×10^{-8}
$k_{a,\gamma}$ (m/s)	3.398×10^{-4}	4.725×10^{-4}	6.332×10^{-4}	7.923×10^{-3}	9.335×10^{-3}	1.077×10^{-2}
K (-)	0.151	0.257	0.618	0.183	0.325	1.000
RMSE (-)	0.005	0.007	0.009	0.010	0.009	0.011
R^2 (-)	0.998	0.997	0.996	0.995	0.996	0.996
SSR (-)	0.109	0.134	0.161	0.123	0.149	0.179
SSE (-)	1.992×10^{-4}	3.601×10^{-4}	6.173×10^{-4}	6.700×10^{-4}	5.574×10^{-4}	8.014×10^{-4}
SST (-)	0.110	0.134	0.162	0.123	0.149	0.180

Figure Captions

Figure 1. Summary of the mathematical model for representing the CSE and UAE of anthocyanins from grape pomace

Figure 2. Experimental and predicted values of anthocyanins concentration at solvent phase for CSE and UAE

Figure 3. Ultrasound assistance impact on the extraction of anthocyanins

Figure 4. Confidence and prediction bands for the anthocyanin concentration at the solvent phase
a. CB and PB for CSE at 45 ºC
b. CB and PB for UAE at 45 ºC

Figure 5. Normal probability plots of residuals
a. Residuals for CSE at 45 ºC
b. Residuals for UAE at 45 ºC

Figure 6. Sensitivity analysis for the anthocyanin extraction yield
a. Washing period of CSE at 65 ºC
b. Slow extraction period of CSE at 65 ºC
c. Washing period of UAE at 65 ºC
d. Slow extraction period of UAE at 65 ºC

Figure 7. Prediction of anthocyanins concentration evolution
a. Concentration at solvent phase for intermediate temperatures at CSE
b. Concentration at solvent phase for intermediate temperatures at UAE

Figure 8. Extraction performance for different operating conditions
a. Time and temperature for obtaining 50, 75 and 90% extraction yield through CSE
b. Time and temperature for obtaining 50, 75 and 90% extraction yield through UAE

Figure
Click here to download high resolution image

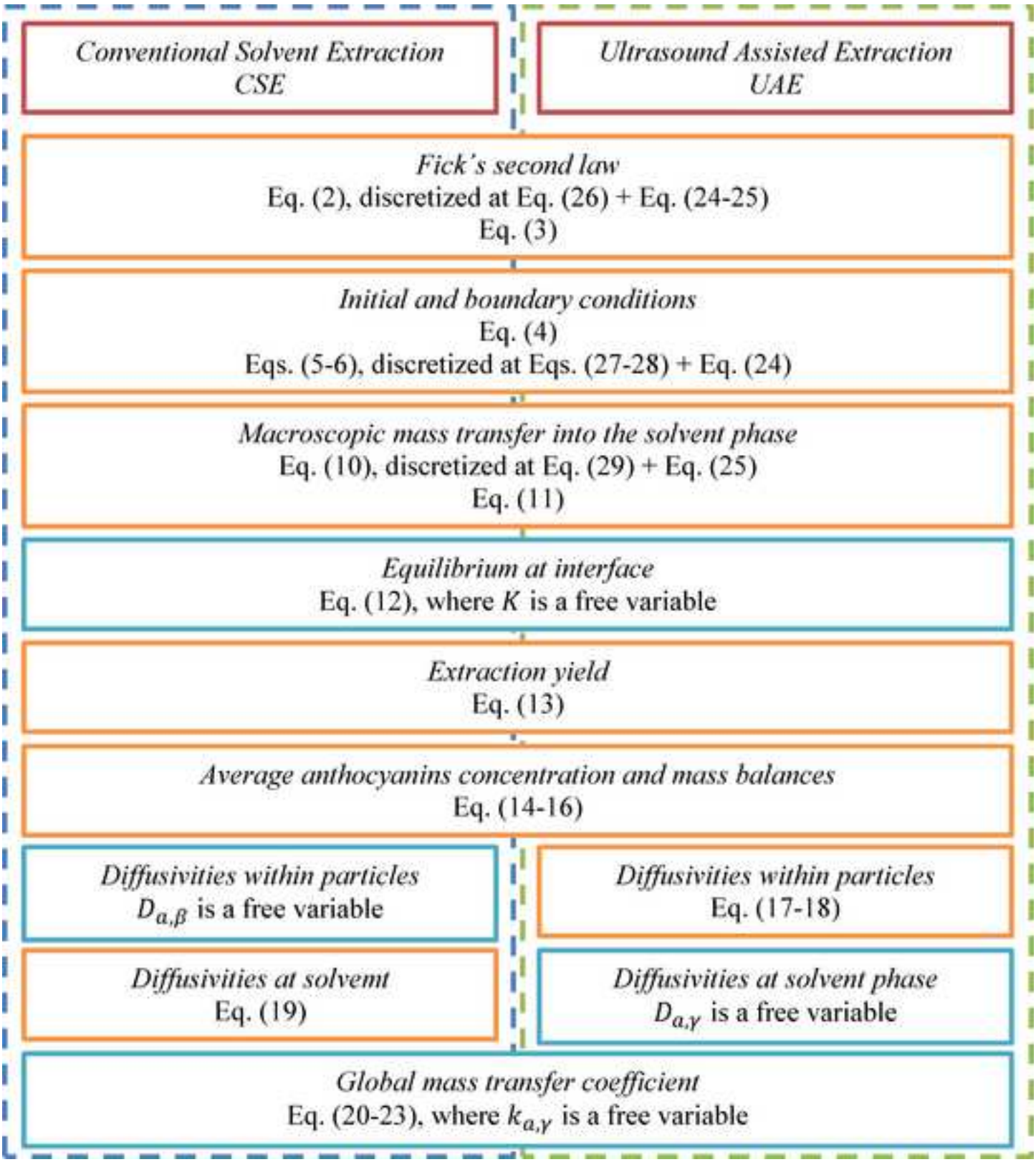

Figure

Click here to download high resolution image

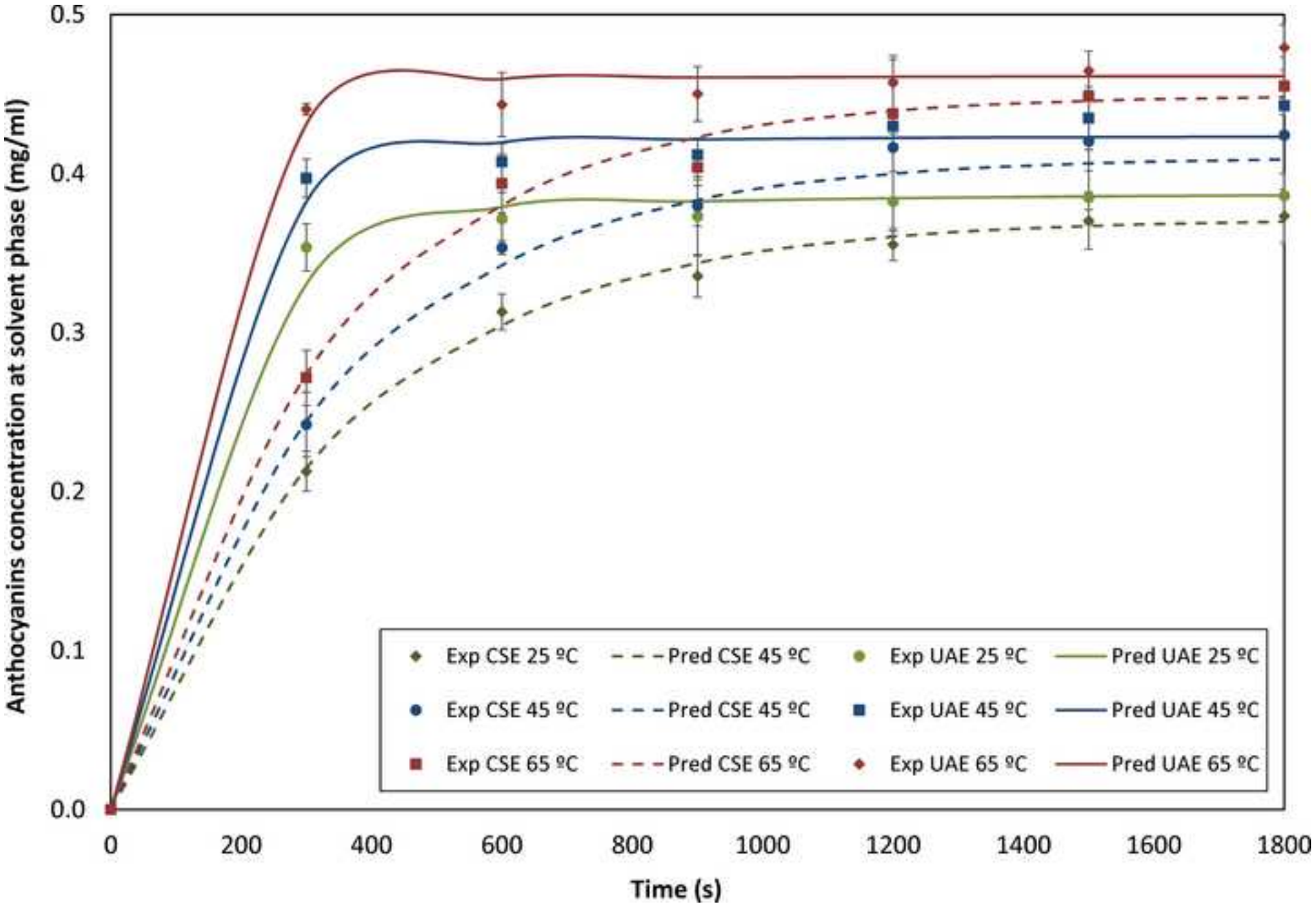

Figure

Click here to download high resolution image

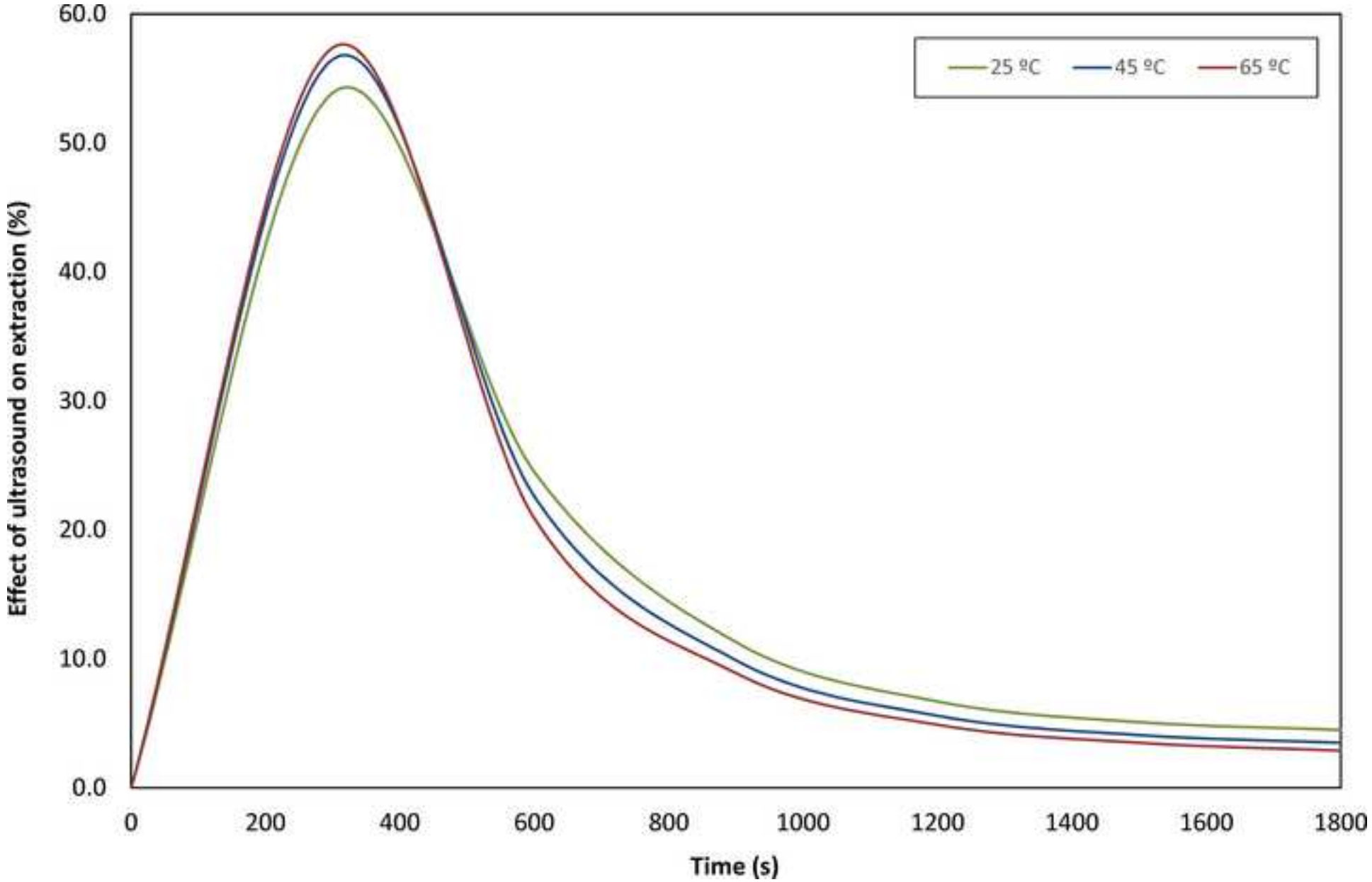

Figure

Click here to download high resolution image

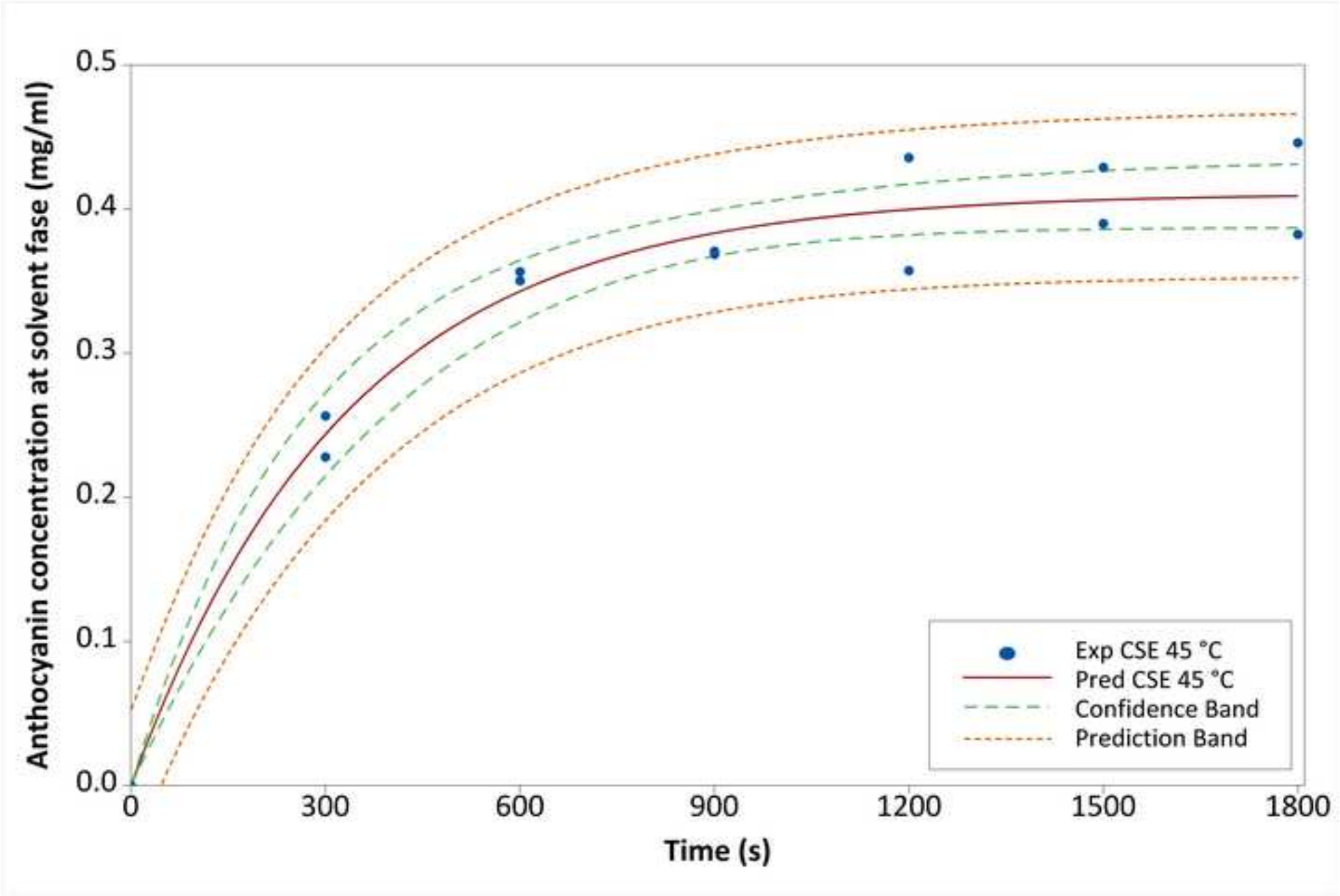

Figure

Click here to download high resolution image

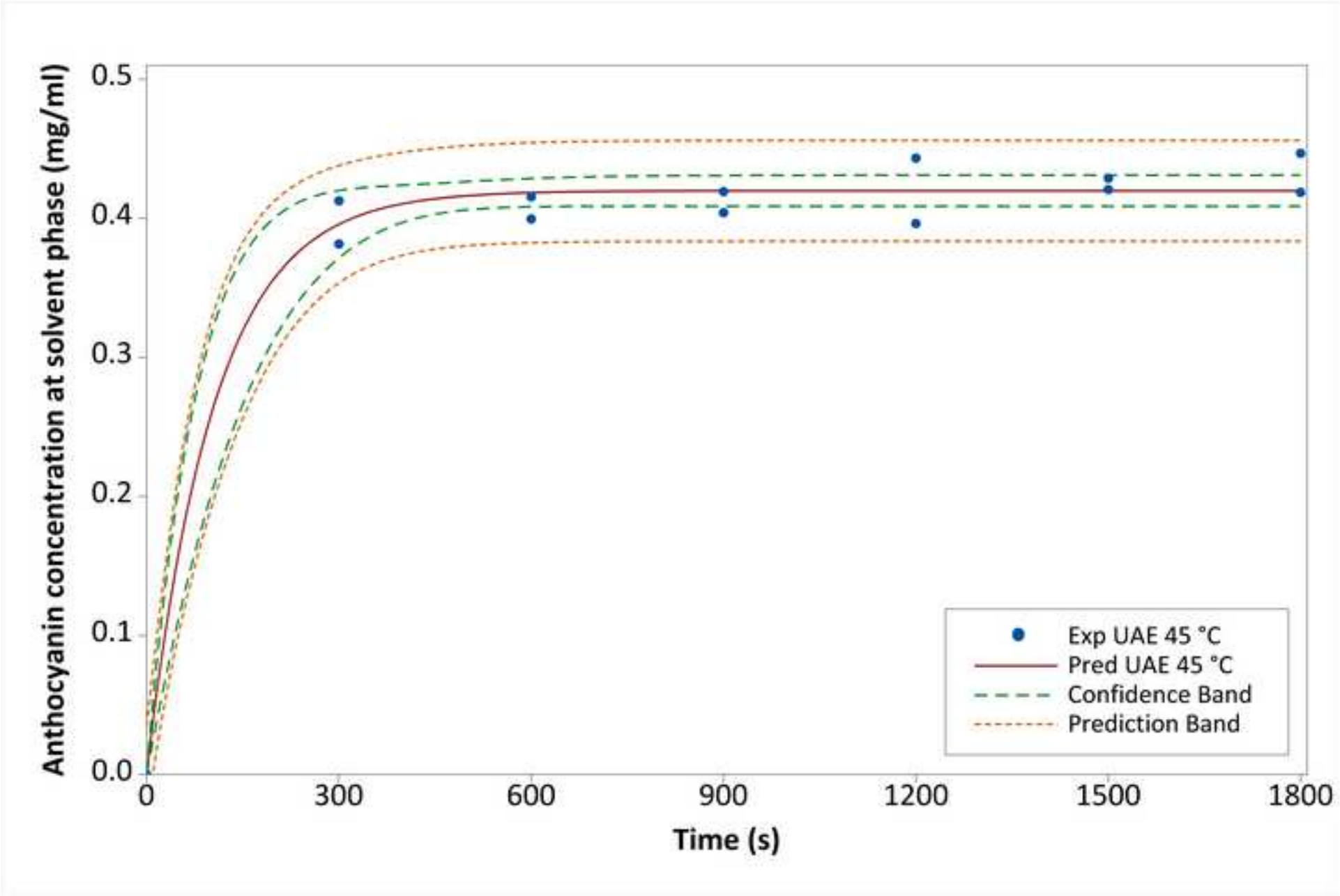

Figure

Click here to download high resolution image

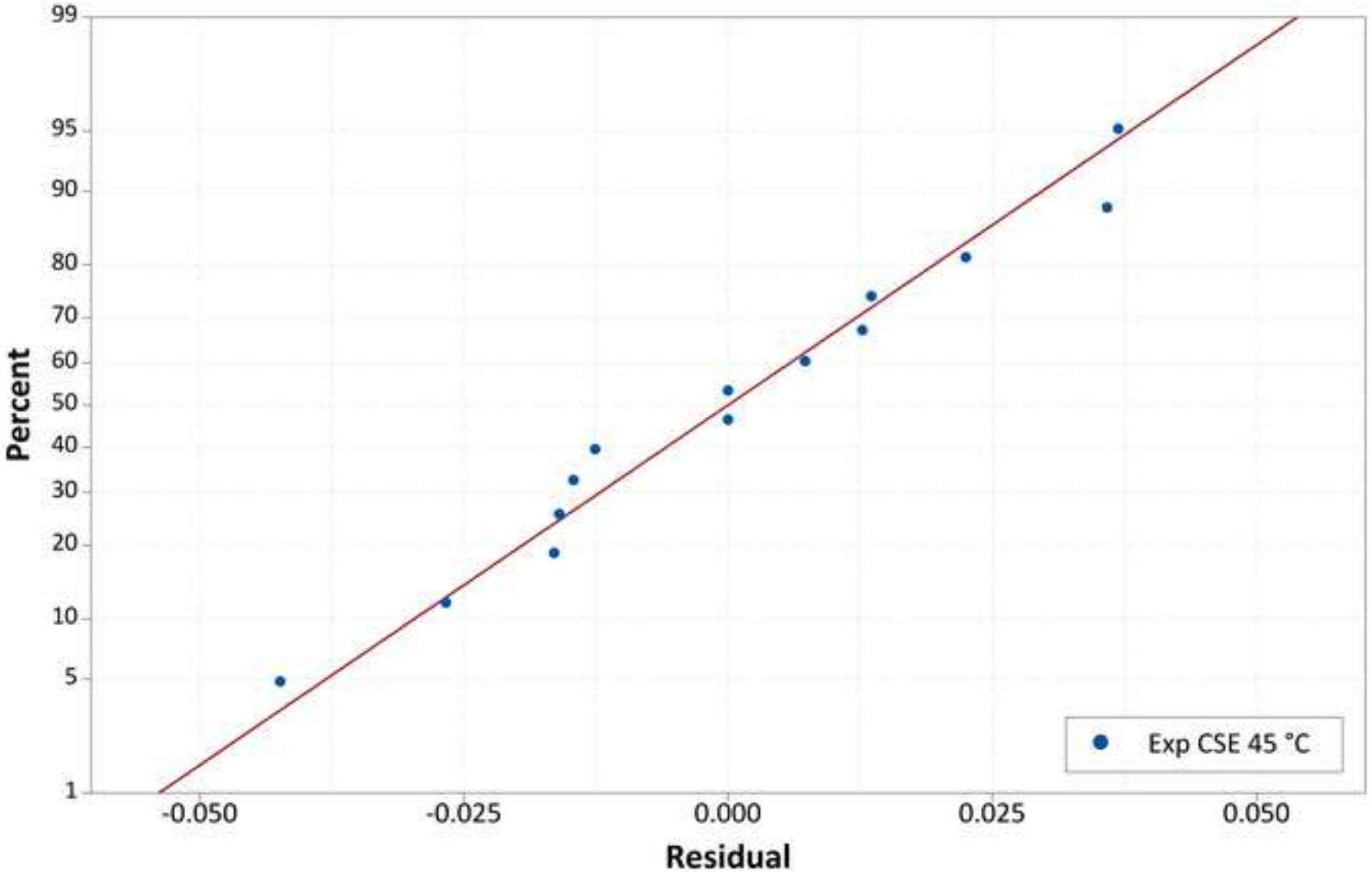

Figure

Click here to download high resolution image

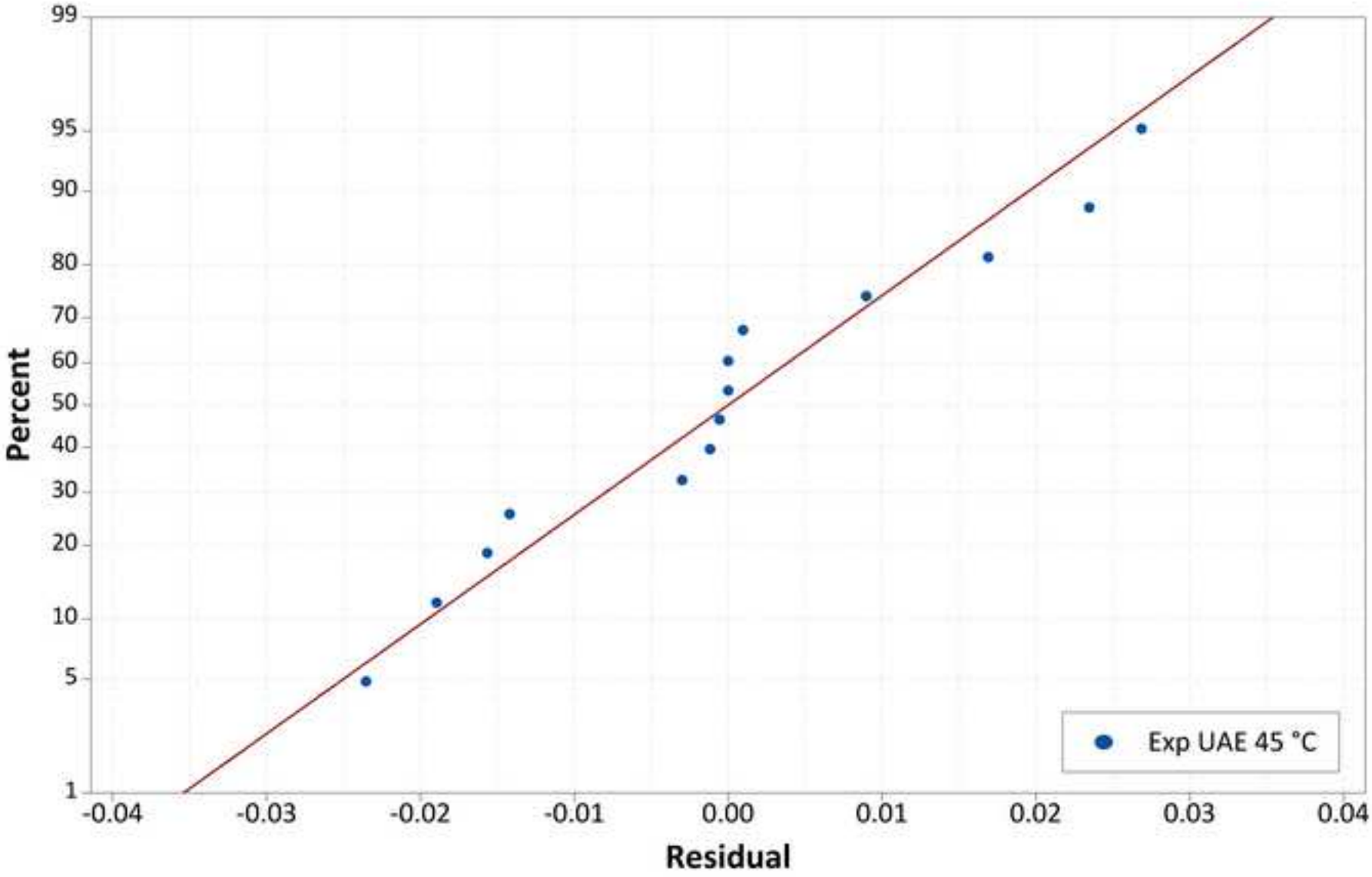

Figure

Click here to download high resolution image

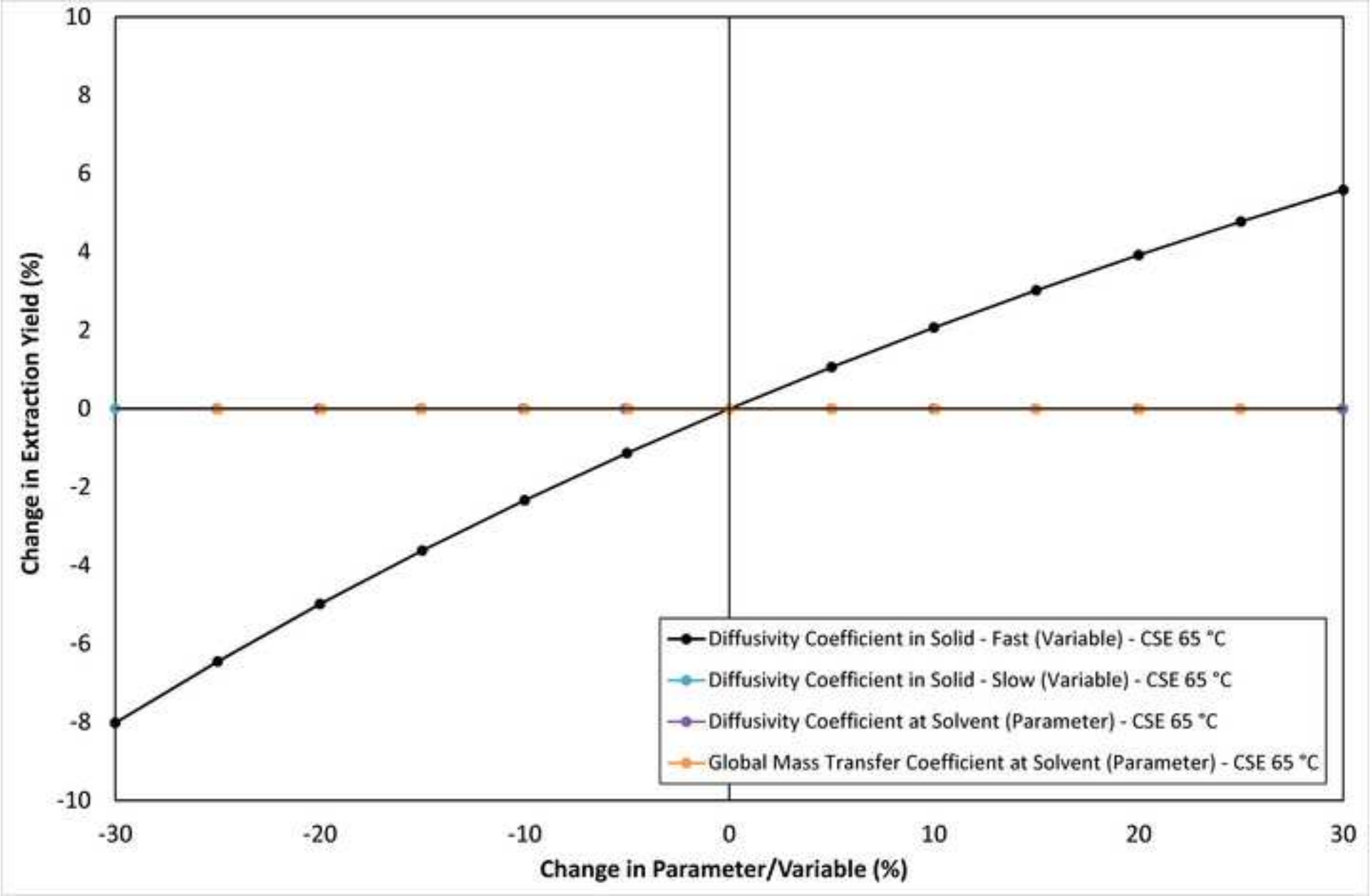

Figure

Click here to download high resolution image

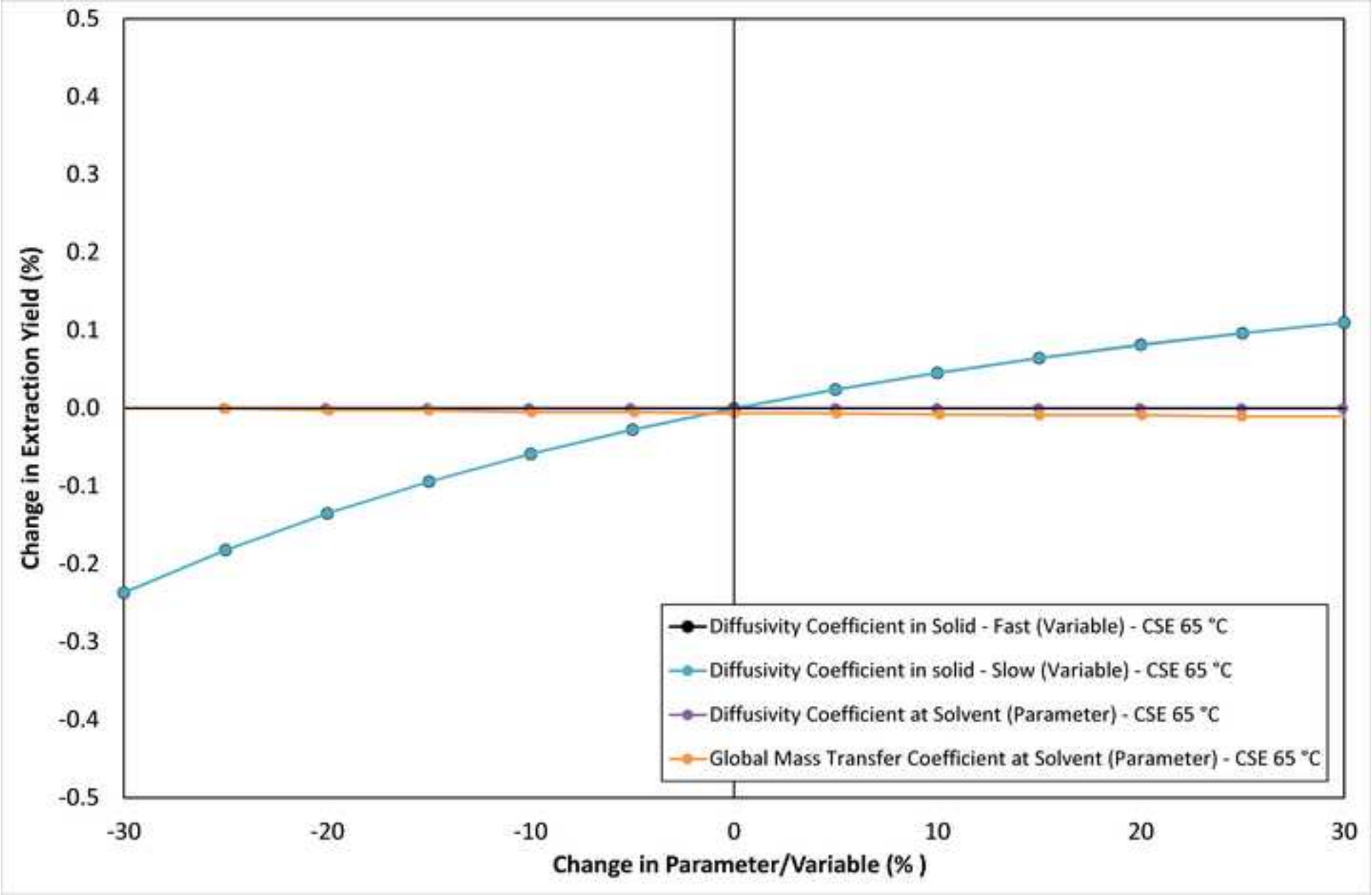

Figure

Click here to download high resolution image

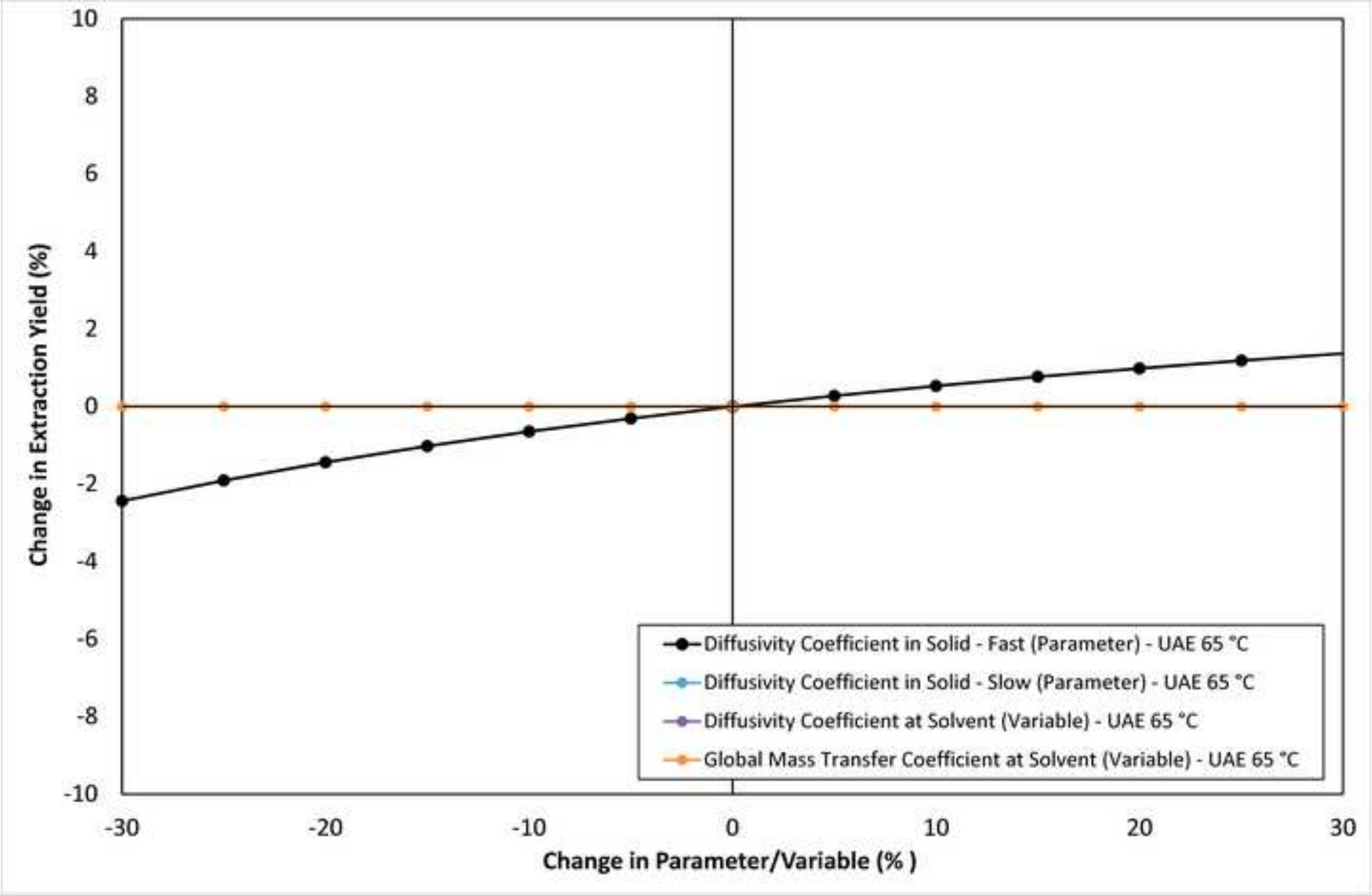

Figure

Click here to download high resolution image

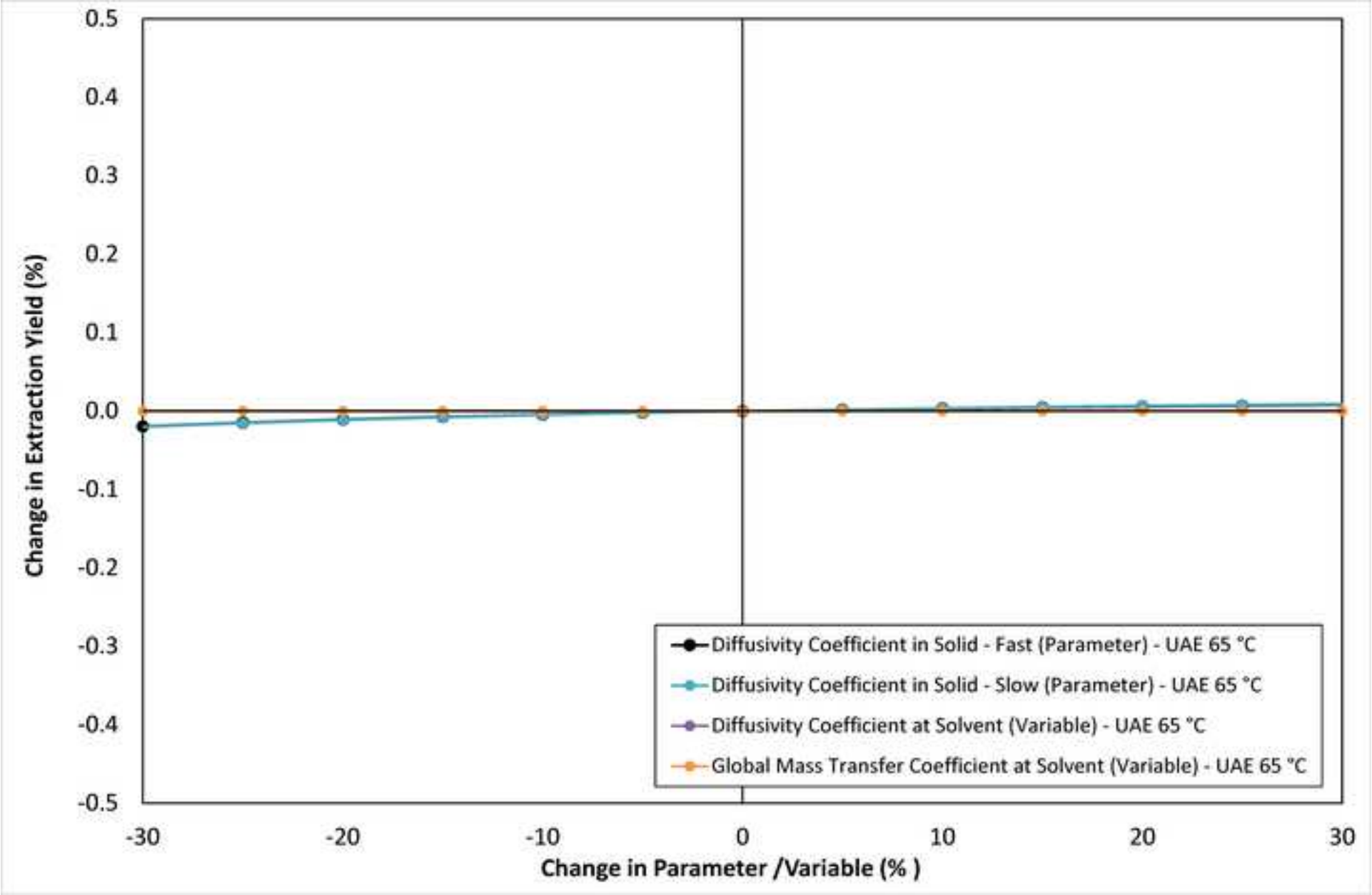

Figure

Click here to download high resolution image

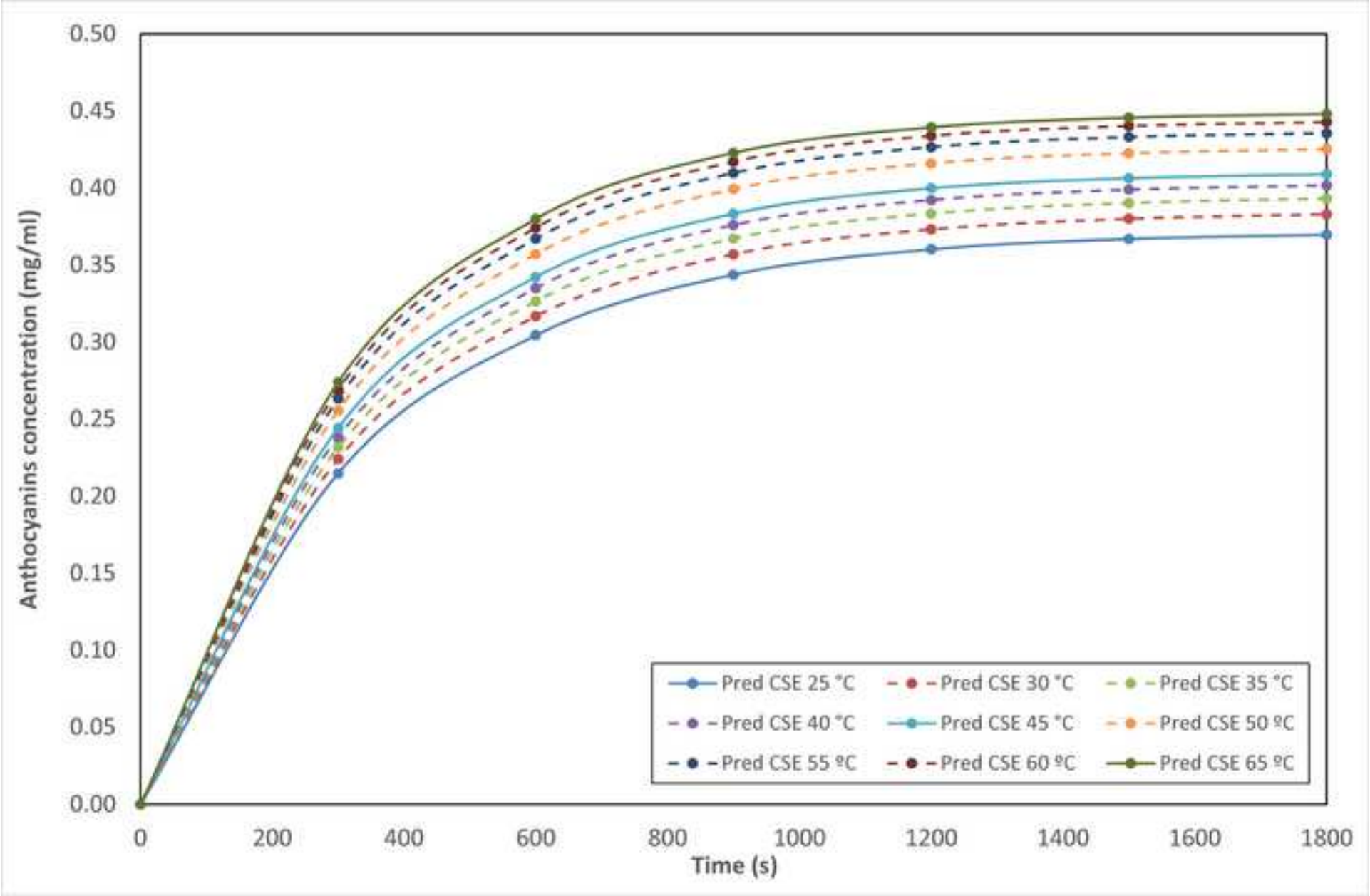

Figure

Click here to download high resolution image

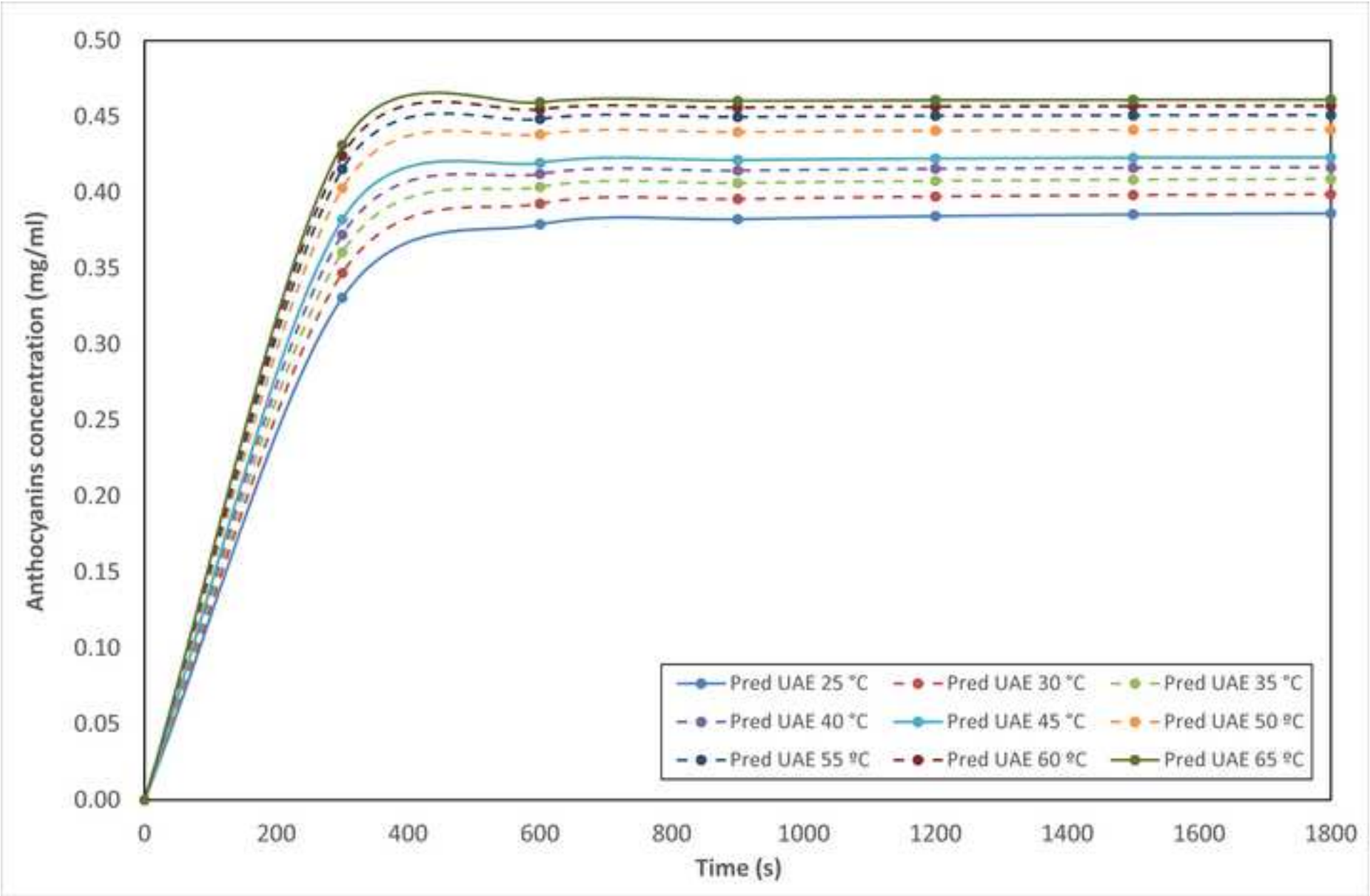

Figure

Click here to download high resolution image

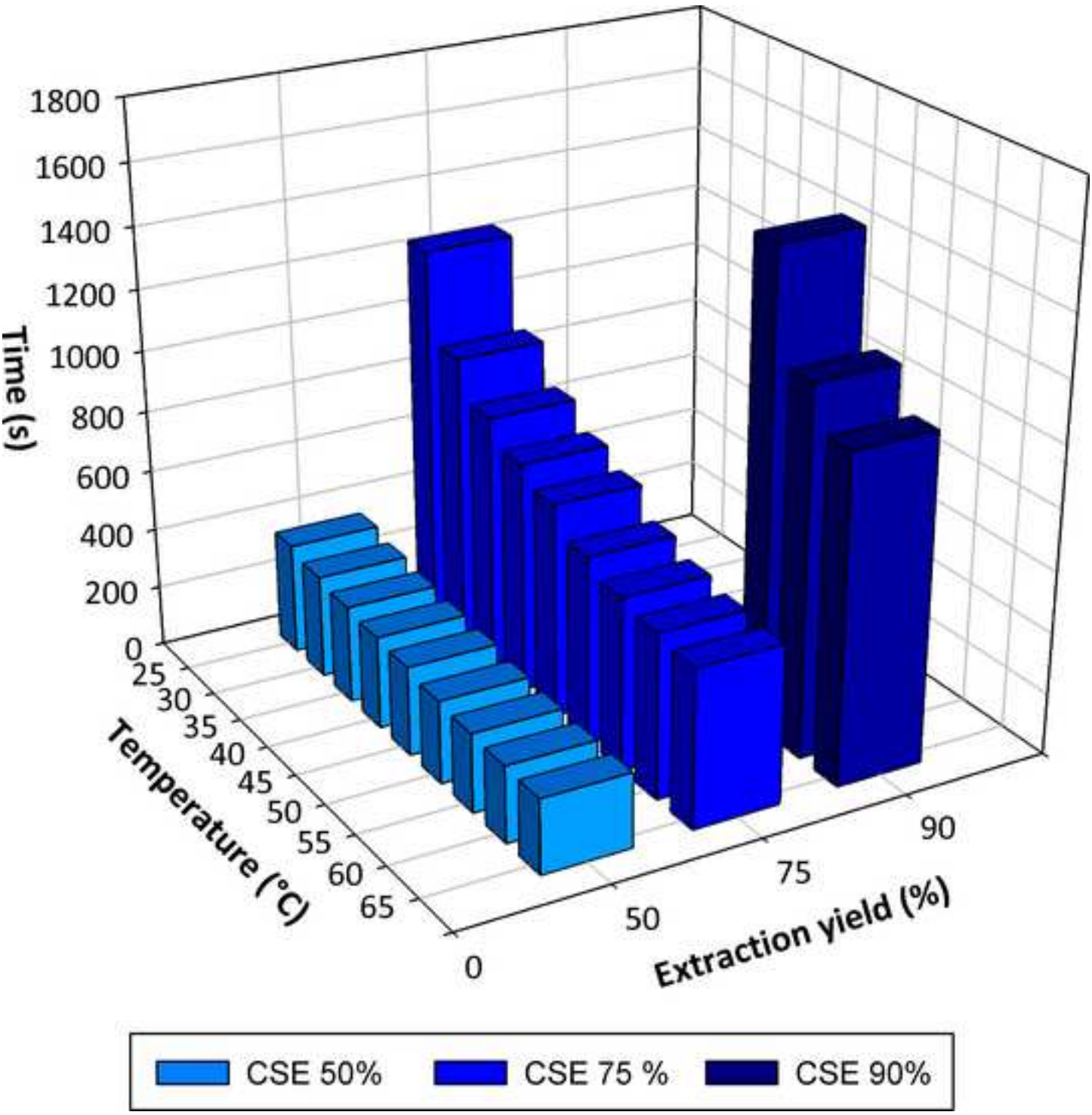

Figure

Click here to download high resolution image